May-Britt Tessem

Metabolic effects of ultraviolet radiation on the anterior part of the eye

Doctoral thesis
for the degree of philosophiae doctor

Trondheim, January 2006

Norwegian University of Science and Technology
Faculty of Medicine
Department of Neuroscience

NTNU
Innovation and Creativity

NTNU
Norwegian University of Science and Technology
Doctoral thesis
for the degree philosophiae doctor
Faculty of Medicine
Department of Neuroscience

ISBN 82-471-7785-4 (printed version)
ISBN 82-471-7784-6 (electronic version)
ISSN 1503-8181

Doctoral theses at NTNU, 2006:22

Printed by NTNU-trykk

Acknowledgements

This work was conducted at the Department of Neuroscience, Faculty of Medicine at the Norwegian University of Science and Technology (NTNU). I thank the staff at my Department for all practical help and colleagues for making a friendly atmosphere in the new Neuroscience building at St. Olavs hospital. This work was funded by the Norwegian Research Council, and additional financial support was received from Lise and Arnfinn Heje`s Fund (Nesoddtangen), Rasmussen`s Fund (Falkenberg, Sweden), the Medical Faculty, NTNU, and the Office of International Relations, NTNU.

During my work with this thesis I have received help, support and encouragement from several people, both professionally and in private life. For this I am eternally thankful to you all. I specially want to thank my supervisor Prof. Anna Midelfart for giving me the opportunity to work in the exiting field of ophthalmology, and my other supervisor Dr. Tone Frost Bathen for introducing me to NMR. You have both been of the utmost importance for my inspiration and eagerness for this work. Dr. Oddbjørn Sæther, you have been of great help with your extraordinary skills in NMR and I want to thank you for always being there to answer my questions. My gratitude goes also to Dr. Øystein Risa for always being helpful in my work, Engineer Trond E. Singstad for always solving practical NMR problems, and my office partner Miroslav Fris for fruitful discussions and making my office a better place.

Special thanks for productive collaboration go to Prof. Jitka Čejkova and colleges at the Department of Eye Histochemistry and Pharmacology, Institute of Experimental Medicine, Academy of Sciences of the Czech Republic in Prague. Prof. Per G. Söderberg, Dr. Stefan Löfgren, Dr. Vino Mody and all colleagues at St. Eriks Eye Hospital, Karolinska Institutet are thanked for excellent hospitality and cooperation during my visit in their laboratory in Stockholm, Sweden.

I am most grateful to my mother and father for always support and encouragement and to my dearest Trond for being a scientific partner, but mostly for love and care at all times. At last but not least I want to thank all of my wonderful friends, I could never have done this without you!

Trondheim 22nd of January 2006

May-Britt Tessem

Summary

Ultraviolet radiation (UV-R) is an environmental factor known to increase the risk of developing an irreversible opacification of the lens (cataract). Increased irradiance of UV-R to the earth because of depletion of stratospheric ozone is of current concern considering cataract formation. Detailed metabolic information from the cornea, lens and aqueous humour might give valuable knowledge on the biochemical processes occurring in the eye after exposure to UV-R, and thereby a better understanding of the mechanisms by which UV-R induces cataractogenesis. The purpose of this thesis was to study metabolic effects of exposure to UV-R on the anterior part of the eye. Effects of UV-B (280-315 nm) and UV-A (315-400 nm) on the aqueous humour, cornea and the lens from animal models were investigated by ^{1}H nuclear magnetic resonance (NMR) spectroscopy. Since the lens is composed of functionally distinct anatomical compartments, with different metabolic activity, biochemical changes in various compartments of the lens were analyzed.

Application of NMR-based metabonomics was effective to analyze metabolic changes in the anterior part of the eye after exposure to UV-R. High-resolution (HR) magic angle spinning (MAS) ^{1}H NMR spectroscopy provided high quality spectra from intact tissue of cornea and lens, and provided important information about metabolic alteration occurring in these tissues after exposure to UV-R. The results from this thesis show that in vivo UV-B radiation affects metabolism of the anterior compartments of the eye. Metabolic changes were observed in aqueous humour, cornea, lens and in the different compartments of the lens. The antioxidants, glutathione and ascorbate, several amino acids, high energetic phosphates, and compounds important for membrane building and osmoregulation were substantially altered after exposure to UV-B radiation. Several biochemical effects such as oxidation, membrane disruption, osmoregulatory problems, lipid peroxidation, problems with cellular signalling and impairment of growth and protein synthesis were suggested. After UV-A exposure, no observable metabolic alterations were found in the anterior part of the eye in the present animal models.

List of papers

I. Tessem MB, Bathen TF, Čejková J, Midelfart, A. Effect of UV-A and UV-B irradiation on the metabolic profile of aqueous humor in rabbits analyzed by ^{1}H NMR spectroscopy. *Invest Ophthalmol Vis Sci*. 2005;46:776-781.

II. Tessem MB, Bathen TF, Čejková J, Midelfart, A. Effect of UV-A and UV-B irradiation on the metabolic profile of rabbit cornea and lens analysed by HR-MAS ^{1}H NMR spectroscopy. *Ophthalmic Res.* 2006;38:105-114. (Published online Desember 22nd, 2005)

III. Tessem MB, Bathen TF, Löfgren S, Sæther O, Mody V, Meyer L, Dong X. Söderberg PG, Midelfart, A. Biochemical response in various compartments of the rat lens after in vivo exposure to UVR-B analyzed by HR-MAS ^{1}H NMR spectroscopy. Submitted to *Invest Ophthalmol Vis Sci*.

Abbreviations

^1H	Proton nucleus
ANOVA	Analysis of Variance
ARVO	Association for Research in Vision and Science
ATP/ADP/AMP	Adenosine Triphosphate/Adenosine Diphosphate/Adenosine Monophosphate
COSY	Correlation Spectroscopy
CPMG	Carr-Purcell-Meiboom-Gill (spin-echo pulse sequence)
DAA	Dehydroascorbate
FID	Free Induction Decay
FWHM	Full Width at Half Maximum
GDP/GTP	Guanosine Di- and Triphosphate
GSH/GSSG	Glutathione, reduced/oxidised form
HR-MAS	High-resolution magic angle spinning
ICNIRP	International Commission on Non-Ionizing Radiation Protection
J/m^2	Physical unit for the dose (1 kJ/m^2 = 0.1 J/cm^2) (1 J = 1 W*s)
JRES	J-resolved spectra
MAD	Maximum Acceptable Dose
NMR	Nuclear Magnetic Resonance
PC1/PC2	The first principal component/the second principal component
PCA	Principal Component Analysis
Phe	Phenylalanine
ppm	Parts per million
PR	Pattern Recognition
$R^{\bullet}$	Free radical species
ROS	Reactive Oxygen Species
SIMCA	Soft Independent Modelling of Class Analogy
T_1	*Spin-lattice* (longitudinal) relaxation
T_2	*Spin-spin* (transverse) relaxation
UNEP	United Nations Environment Programme
UV-A	Ultraviolet A Radiation (315-400 nm)
UV-B	Ultraviolet B Radiation (280-315 nm)
UV-C	Ultraviolet C Radiation (100-280 nm)
UVI	Ultraviolet index (global solar)
UV-R	Ultraviolet Radiation
WHO	World Health Organization
WMO	World Meteorological Organization

Contents

INTRODUCTION: ULTRAVIOLET RADIATION AND THE EYE

Ultraviolet radiation

Biological effects

All human beings are exposed to ultraviolet radiation (UV-R) from the sun, and an increasing number of people are exposed to artificial sources of UV-R used in industry, commerce and recreation. Ultraviolet radiation has the ability to damage organic molecules such as nucleic acids, proteins and other molecules within the living cell, which absorb UV-R and may be structurally altered, cleaved or react with other molecules. Such alterations can cause changes in cell function, mutations or death of cells.[1]

How much UV-R reaches the earth?

The ozone layer is spread out between 10 and 50 km in the stratosphere and absorbs the most energetic and harmful UV-R from the sun. The UV-R region covers the wavelength range between 100-400 nm and is divided into three bands: UV-A (315-400 nm), UV-B (280-315 nm) and UV-C (100-280 nm). As sunlight passes through the atmosphere, all UV-C wavelengths and approximately 90% of UV-B are absorbed by ozone, water vapour, oxygen and carbon dioxide. The less energetic UV-A radiation is not absorbed by ozone and reaches ground level without much attenuation through a clear atmosphere. Therefore, the average UV-R reaching the surface of the earth is largely composed of UV-A (97%) and a small component of UV-B (3%). The level of UV-R reaching the earth is however strongly influenced by environmental factors such as sun height, season, latitude, altitude, ozone and cloud cover.[1]

Ozone depletion and increased influx of UV-R

Ozone might be destroyed by industrially produced chlorine- or bromine-containing substances such as chlorofluorocarbons. These substances decompose by high-energetic UV-R in the stratosphere, causing reactive chlorine and bromine to be released. A depletion of stratospheric ozone has over the last 2 decades been discovered in temperate and polar climate zones.[2,3] The consequence of a depleted amount of the ozone layer is an increased flux of UV-R at the surface of the earth, and especially UV-B radiation. This will enhance photochemical reactions in organic

molecules and increase the corresponding biological effects. Health consequences believed to be caused by UV-R include skin cancer, cataract and cellular immunity.

Cataract

What is cataract and what are the risk factors?

Cataract is defined as an opacity of the lens of the eye, and when this opacity interferes with vision, a clinical cataract is present.[1] There are three major types of cataract; cortical, nuclear and posterior subcapsular opacities, where each type has its own pathogenic changes and age distribution. Cataract is a multifactorial disease which has several possible risk factors as exposure to ultraviolet radiation, smoking, diabetes, alcohol, diet, diarrhea, age, low antioxidant intake, steroid use and other medications.[4] The primary modifiable environmental risk for cortical cataract is the ocular exposure to UV-B. The World Health Organization estimates that as many as 20% of blind patients have developed cataract from UV-R exposure.[5] In recent years, genes have been demonstrated as another important risk factor of cataractogenesis.[6,7] A new study states a significant genetic correlation for age-related cortical cataract but not posterior subcapsular cataract[6]. However, the precise mechanism of this control remains to be explained.

Treatment and expenses

Age-related cataract is the leading cause of blindness in the world today, and as the world's population ages, this will become a significant global problem. In Australian studies, the prevalence of cataract is found to double after the age of 40.[8] Over the next 20 years, the number of people over 65 years old will more than double,[9] and the need for cataract treatment in the near future will increase accordingly. Currently, surgery is the only available treatment for cataract, involving replacement of the opaque lens by a plastic one.[10] Surgery is effective to cure cataract blindness, but the outcome is dependent on the availability of experienced surgeons and the quality of the postoperative care.[11] Even with high quality surgery, the expenses are very high considering that cataract is a frequent surgical intervention. Cataract surgery is among the most frequently performed procedures world wide, with an annual cost of over $3 billion in the United States.[12] The future world challenge will be to develop strategies to prevent or delay cataract formation. Delaying the onset of cataract by 10 years would decrease the need for surgery by 50%.[13]

Epidemiological studies and UV-R

Although it is difficult to determine ocular UV-R exposure in different climates and in individuals with different behaviour, the epidemiological studies clearly demonstrate that UV-R is an aetiological factor in cataractogenesis. The majority of the epidemiological studies support an association between UV-B exposure and the development of cortical cataract and perhaps posterior subcapsular cataract, but not nuclear cataract.[14,15] These epidemiological studies justify the implementation of public health campaigns to raise awareness of the risk of cortical cataract due to UV-B exposure.[14] Recent epidemiological studies have suggested that sunlight may have a role in the brown coloration typical for age-related nuclear cataract[10]. The transparent lens becomes yellow with age and the reason for this coloration is unknown. Preliminary studies have shown that specific UV-filters (protective agents in the lens) become more susceptible to UV-R with age and might cause this lens coloration.[10]

Animal models and UV-R

Several animal models and biochemical studies show that UV-B irradiation causes cataractogenesis[16,17] (Fig. 1). This evidence is found in both *in vivo* and *in vitro* experiments.[18] Most studies are performed on cataract caused by acute short-term UV-B exposure, but there are also experiments employing repeated irradiation over longer periods of time.[19] The UV-B action spectrum for the pigmented rabbit was presented by Pitts et al., who showed that a wavelength of 300 nm is most cataractogenic.[16] The effects of UV-A radiation (315-400 nm) and development of cataract are still highly debated.[20] In recent years, the longer wavelengths of the UV-A spectrum are in animal models accepted as a risk factor for damaging lens enzymes, crystallines and cell membranes.[21-23] In cultured rabbit lens epithelial cells, both UV-A and UV-B radiation caused cell death, decreased viability and increased lipid peroxidation.[18] In the cornea, which is a major protective layer against UV-R, antioxidant enzyme systems is found to change after exposure to UV-A and UV-B.[24] Knowledge about the effect of UV-A radiation on metabolism of the anterior part of the eye is scarce.

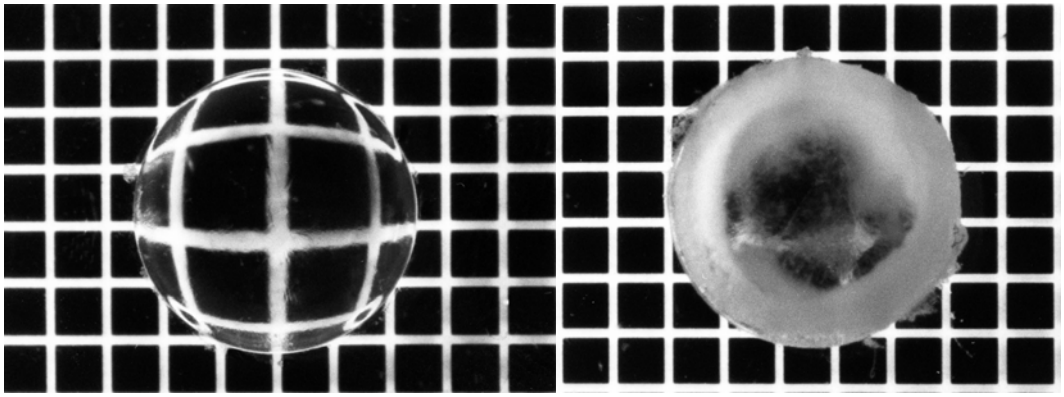

Figure 1. Macroscopic appearance of isolated lenses from six-week old Sprague-Dawley rats. The left one is an unexposed lens with a clear appearance. The right one has developed severe opacities one week after in vivo exposure to UV-B (8 kJ/m^2). Courtesy of Dr. Xiuqin Dong.

Transferring animal models to human research

A series of investigations has proven that UV irradiation of the rat eye provides a reliable and reproduceable cataract model with several considerable advantages over other experimental cataracts. UV irradiation experiments are closer to natural circumstances of senile cataract formation than in cases of X-ray, naphthalene or experimentally induced diabetic cataract models.[25] However, animal models simulate mainly acute damages, even if relatively long periods with repeated exposure are chosen. In contrast, the UV stress on the intraocular tissues in humans spans years or decades. The great challenge in UV-R and cataract research using animal models is to create a model that reflects the human responses to UV-R. The general lens structure, growth pattern and the proteins are found to be comparable in rat and human lens.[26] Animal models can therefore contribute to our knowledge about lens biochemistry and pathobiochemistry.

Human ocular UV-exposure

How much UV-R reaches the eye? Sun protection

Only a fraction of the solar UV-R will reach the human eye on a sunny day. The facial geometry with eyebrows and eyelids protect the eye from direct solar radiation, and the squinting reflex is important for reducing the ocular UV-dose.[27] Other behavioural factors that influence ocular exposure to UV-R are the use of different devices for sun protection, such as a brimmed hat or sunglasses.[27] The protective ability of sunglasses

is dependent on the type of glass, size, shape and the distance from the eye. This is shown in a study of lateral ocular UV-R exposure, called the Corroneo effect, where temporal rays can focus in a 20-fold concentration at the nasal limbus. (Fig. 2) Corroneo proposed that the predominance of cortical cataract in the nasal quadrant can be explained by this specialized geometrical exposure factor.[28] This hypothesis is consistent with the findings of the Island Reykjavik study and the Beaver Dam study which showed initial cortical cataract in the inferior nasal quadrant.[14,29] These findings suggest the need of improved ocular protective devices, especially with improved lateral protection.

Measurements of human UV-R exposure

Several attempts have been made to measure human ocular UV-R exposure, but the amount of influencing factors such as personal behaviour and climate make such measurements difficult. Rosenthal et al. defined the ocular-to-ambient exposure ratio as the relationship between incoming UV to the earth and ocular exposure.[30] The ratio was between 2% and 17%, depending on clothes, working conditions and time of the year.[30] The exposure ratio was determined by placing UV-sensitive film between the eyes of outdoor workers. Quantification of lifetime UV-R exposure in free-living populations is extremely challenging because the ocular dose is dependent on the personal behaviours such as time spent outdoors, the use of sun protection and other lifestyle related factors through a whole life.

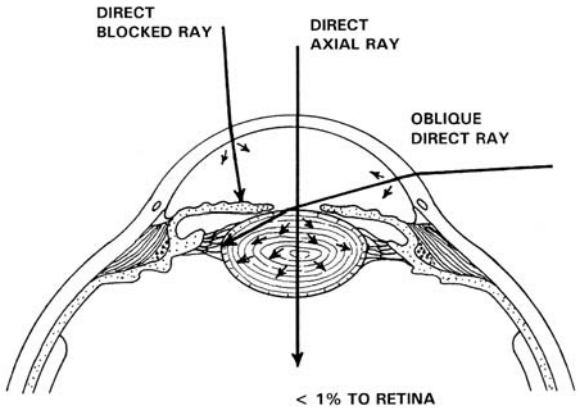

Figure 2. The Corroneo effect: an increased concentration of UV energy absorbed in the vicinity of the nasal limbus (reprinted from Sliney 2001 with permission from Elsevier Ltd).[27]

Social aspects and lifestyle

Social aspects and lifestyle have in recent decades changed rapidly especially in northern Europe. Sun-bathing and holidays spent in warmer and tropical climates increase the total UV-R exposure substantially. On the other hand, increased work indoors has recently decreased total UV-R exposure, but this might lower the tolerance to UV-R.[26] These are new and challenging facts that will influence ocular UV-R exposure in a different way than in previous years. In addition, an increased life-expectancy will also influence the total UV-R exposure to the eye.

UV-R exposure to the structures of the anterior part of the eye

To understand the effect of UV-R exposure to the anterior part of the eye, knowledge of the anatomy, transmission and absorption properties of the tissues is important. When UV-R reaches the eye, the proportion absorbed by different structures depends on the wavelength of the radiation (Fig. 3).

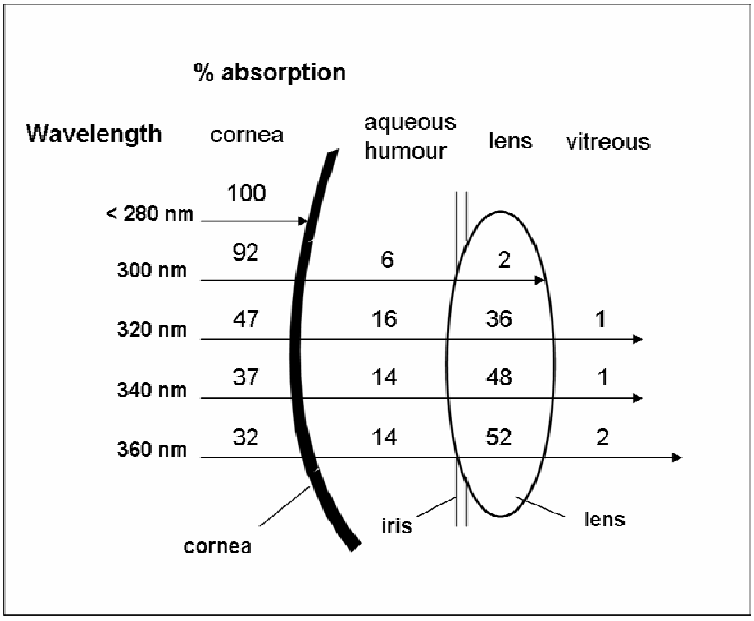

Figure 3. Absorption of different wavelengths of UV-R by the structures of the anterior eye (Based on data from Boettner and Wolter 1962).[31]

The Cornea

The shorter UV-B wavelengths are absorbed at the highest rates by the cornea (92% at 300 nm, Fig. 3). The cornea is the major light-refractive structure in the eye. The human cornea consists of five different layers; epithelium, Bowman`s membrane (basal lamina), stroma, Descemet`s membrane and endothelium (Fig. 4). The corneal stroma constitutes about 90% of the total corneal thickness and is highly organized with collagen fibers in a pattern that makes the cornea transparent.[32,33] The epithelium has cells that undergo rapid turnover, and the endothelium is an active ion pump maintaining hydration in the stroma. All these mechanisms are important to maintain transparency. Wavelengths below 290 nm are almost completely absorbed by the corneal epithelium and do not penetrate to the deeper underlying structures of the eye.[34] This confirms that the epithelium protects deeper, underlying ocular structures against UV-R in the 280 nm range. However, depending on UV-R dose, these short wavelengths cause apoptosis and loss of corneal epithelial cells.[35] UV-R with longer wavelengths (310 nm) results in much deeper corneal damage, with apoptosis and disappearance of keratocytes (source of stromal collagens and proteoglycans), formation of cells with nuclear fragmentations as well as epithelial damage.[35,36] Acute exposure of the mammalian eye to an above threshold-dose of UV-R results in the development of photokeratitis ("snowblindness") after a few hours.[1,16] Photokeratitis is an acute reversible radiation-induced injury of the corneal epithelium. Chronic exposure to UV-R may be associated with several eye diseases, including pterygium (a non-malignant growth on the conjungtiva), climatic droplet keratopathy (degenerative condition of the corneal stroma)[37] and climatic proteoglycan stromal keratopathy.[38,39]

When studying effects of UV-R on corneas from experimental animals, it is important to be aware of variance in corneal thickness,[15,26] which results in different corneal transmittance of UV-R. The transmittance at 300 nm varies from 32% in the rat, 13% in the rabbit and 10% in humans. Transmittance of a longer wavelength (380 nm) varies from 76% in the rat, 71% in the rabbit and 63% in humans.[15] At 300 nm, the transmittance of the rabbit cornea and the human cornea are very similar.[15] Therefore,

rabbits seem to be the closest of the laboratory animals mentioned for use in comparative studies investigating effects of UV-R to the anterior eye.

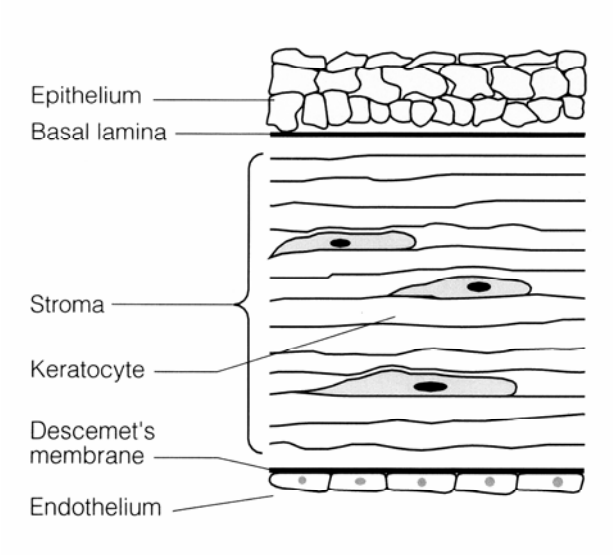

Figure 4. The different layers in the human cornea (reprinted from Forrester et al: The eye, 2002 with permission from Elsevier Ltd).[33]

The aqueous humour

The aqueous humour is a transparent fluid which fills the anterior and the posterior chamber in the anterior segment of the eye and is formed by blood plasma and secreted by the nonpigmented ciliary epithelium. It contains all the essential nutrients for supplying the avascular lens and cornea, and also removes the waste from these tissues. To maintain optical clarity, the fluid has a very low concentration of proteins.[32] The composition of the aqueous humour is suggested to play an important protective role against UV-A and UV-B irradiation into the lens.[40] The aqueous humour seems to act as a UV-filter, mainly related to its high ascorbate (vitamin C) concentration[41]. Some amino acids might in addition contribute to the UV absorption.[40] The aqueous humour absorbs 6-16% of the incoming UV-R between 280-360 nm (Fig. 3).

The lens

The lens is an avascular transparent crystalline tissue enclosed in a basement membrane called the lens capsule. The transparency of the lens is dependent on the regular organisation of its cells and proteins, and the high protein content and unique arrangement of structural fibers provides the refractive index necessary to focus images

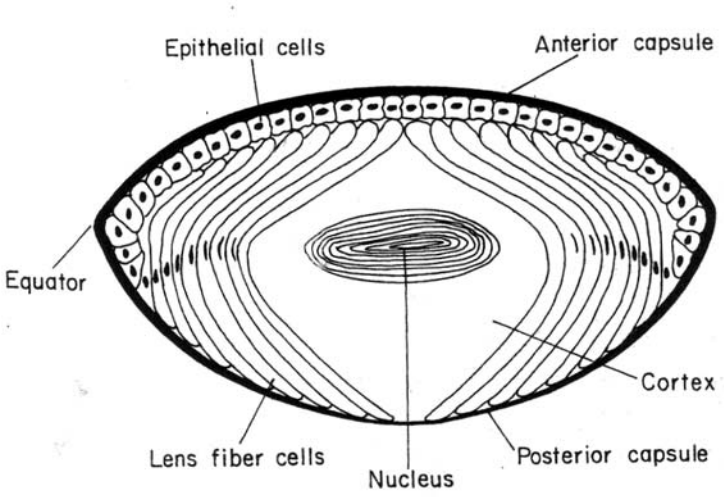

Figure 5. The mammalian lens (Reprinted from. Berman: Biochemistry of the eye. 1991 with permission from Springer).[42]

on the retina. The lens structure is formed by two different cell types; the epithelial cells, on the anterior surface underlying the capsule, and the fiber cells that occupy the rest of the lens and comprise the major cellular component of the tissue. From embryo and throughout life, the epithelial cells undergo mitosis at the equator and differentiate into elongated fiber cells (Fig. 5). The fiber cells differentiate further into mature fiber cells where there is a loss of nuclei and other intracellular organelles. The new fiber cells are laid down as concentric layers on previously formed fiber cells, and thus the nucleus of the lens contains the oldest cells and cortex the newest ones. In the nucleus, there is no protein turnover, and most, if not all, of the protein synthesis occurs in the epithelium and in developing fiber cells.[33,43,44]

The human lens contains chromophores, or UV filters, which absorb UV-R between 295-400 nm and transmit wavelengths longer than 400 nm to the retina (Fig. 3). The absorption of the normal lens increases with age due to a progressive accumulation of age-related chromophores. This provides an effective filter of near-UV and short wavelength visible light for the retina. The absorptive properties are found to vary drastically with age in human lens.[15] The absorption of UV radiation is 2% at 300 nm and 52% at 360 nm (Fig. 3). A small fraction of the UV-B wavelengths will reach the

lens, and these wavelengths are found to have higher potential to damage lens transparency than the UV-A radiation. However, the effects of UV-A radiation on the lens and the development of cataract are still debated.[20-23]

Topography of lens metabolism

Hockwin et al. reviewed cataract research in the 20th century and discussed problems and misunderstandings in several studies.[45] The main question was why cataract research was not able to solve more problems after a substantial effort and financial input. One of the critical points in this discussion was the topography of lens metabolism in biochemical studies. Homogenisation of the total lens has usually been part of the protocol in the past. The recorded data are therefore an average of the compounds analysed in the homogenized lens tissue. Different biochemical activity between the different compartments of the lens is important when studying biochemistry of lens pathology. The Hockwin study states the importance of performing future biochemical analysis on the different compartments of the lens. New and challenging practical problems such as lens division and how to obtain enough material for these biochemical analyses are therefore in focus for lens research.

UV-R dose (exposure limits)

To protect the world population against UV-R induced damages to the eye, it is important to have research data that can propose exposure limits for UV-R. The global solar UV index (UVI) is a simple measure of the UV radiation level at the earth's surface. It has been designed to indicate the potential for adverse health effects to encourage people to protect themselves. The UVI was developed through an international effort by the World Health Organisation (WHO) in collaboration with the United Nations Environment Programme (UNEP), the World Meteorological Organisation (WMO), the International Commission on Non-Ionizing Radiation Protection (ICNIRP), and the German Federal Office for Radiation Protection.[5] The current threshold doses for UV-R induced cataract, defined by the ICNIRP is based on the total literature on experimental and clinical experience. UV-R exposure in the spectral region of 180 to 400 nm upon the unprotected eyes should not exceed 30 J/m^2

(0.003 J/cm^2).[46] The UV-R exposure should be quantified in terms of an irradiance *E* (W/m^2 or W/cm^2) for continuous exposure or in terms of a radiant exposure *H* (J/m^2 or J/cm^2).[46] In the pigmented rabbit, the estimated threshold dose for permanent damage of the tissue was determined to 0.75 J/cm^2 for the lens and 0.055 J/cm^2 for the cornea at 310 nm.[16] At 315 nm the threshold for the lens was 4.5 J/cm^2 and 2.25 J/cm^2 for the cornea.[16] In the albino rat, Söderberg et al. found a maximum acceptable dose (MAD) of 2.2 kJ/m^2 (0.22 J/cm^2) for toxicity of UV-R at 300 nm.[47]

Biochemical effects of UV-R exposure to the anterior part of the eye

Detailed metabolic information can give valuable insight into biochemical processes in an organism. Metabolic studies of tissues from the anterior part of the eye may be helpful in understanding the underlying photobiochemical processes of damage to cornea and lens by UV-R. The constituents of the aqueous humour reflect the metabolic processes within the eye, and thus determination of the various metabolites in aqueous humour is useful in elucidating the pathogenesis of UV-R exposure and development of cataract.

Antioxidants

The eye is an organ which is relatively unprotected and is constantly exposed to damage by sunlight, oxygen, various chemicals and pollution. Each of these threats result in generation of highly reactive oxygen species (ROS) or various free radical species ($R^{\bullet}$), who readily react with other molecules and contribute to ocular damage and diseases. Antioxidants prevent the oxidation of other molecules, and are therefore of special interest when studying biochemical effects of UV-R exposure to the eye. Oxidants or sensitizers present in eyes of diurnal animals include hydrogen peroxide (H_2O_2), singlet oxygen, superoxide anion, hydroxyl radical, tryptophan and its oxidation products and NAD^+. The most important protection against these oxidants in the eye is the water soluble antioxidants ascorbate (vitamin C) and glutathione (GSH).[48]

Ascorbate is suggested to be a significant antioxidant in ocular tissues, protecting the eye from damages caused by ROS. Ascorbate accumulates in ocular tissues of diurnal

animal species at higher concentrations (0.5-2 mM) than in the plasma (0.03-0.2 mM).[48] When ascorbate interacts with free radicals, the the ascorbyl free radical is produced. The ascorbyl free radical may spontaneously decay by the loss of an unpaired electron to form dehydroascorbate (DAA). The ascorbyl free radical may be converted to ascorbate by the enzyme ascorbyl free radical reductase. DAA may be converted to ascorbate chemically by GSH or by an enzymatic process involving dehydrascorbate reductase. In the absence of reducing equivalents, DAA may decay in a irreversible process to diketogulonate (2,3-DKG) which is very unstable and degrades further to oxalate and CO_2.[49] (Fig. 6). Ascorbate is found to act as an UV filter protecting the eye from radiation damage.[40] High levels are detected both in the aqueous humour[40] and in the corneal epithelium of diurnal animals.[50] Ascorbate seem to be involved in this filtering process in three different ways: absorption, fluorescence-mediated ray transformation from energy rich UV to less potent UV waves and fluorescence reduction.

Reduced *glutathione* (GSH) is a highly concentrated antioxidant in the lens, vital for maintenance of lens transparency. Concentrations as high as 12-15 mM have been found in lens tissue.[48] GSH detoxifies damaging oxidants such as H_2O_2 and has hydroxyl radical-scavenging function in the lens epithelial cells. In the lens nucleus however, GSH is found to be almost non-existent.[51] Risa et al. have earlier detected a significant decrease in GSH concentrations in whole lenses after exposure to UV-B radiation.[52]

Amino acids

Amino acids are the basic structural building units of proteins. Some of the 20 standard amino acids are called essential amino acids because they cannot be synthesized by the body, but instead must be acquired from food. In previous studies from our laboratory, several amino acids, both essential and non-essential, were detected in tissue extracts from cornea, lens and directly in aqueous humour by ^{1}H NMR spectroscopy[53-55] and

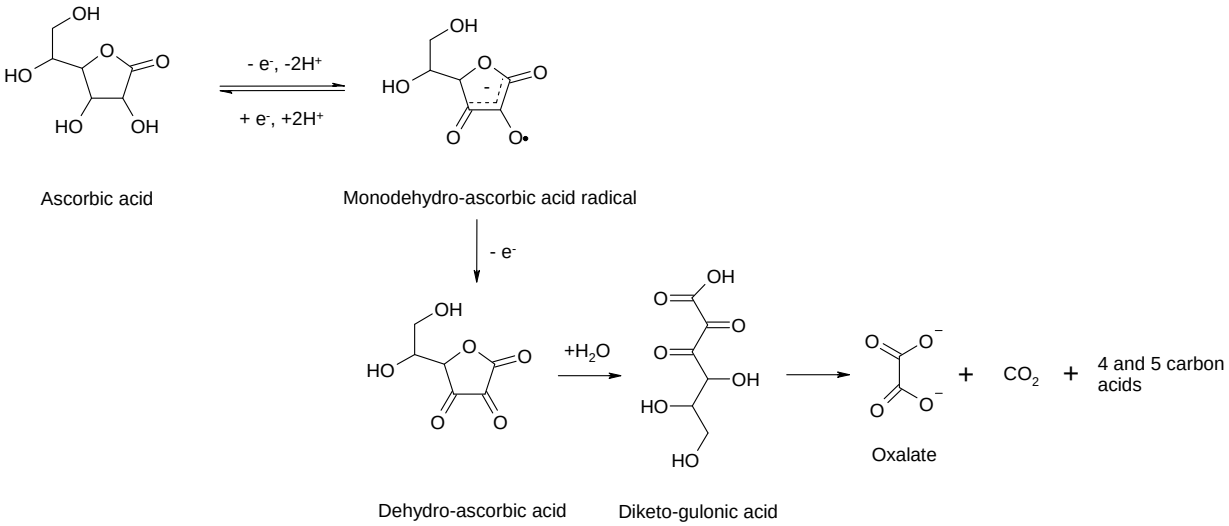

Figure 6. Degradation of ascorbic acid (adapted from Nishikawa and Kurata).[56]

later in intact tissue samples by HR-MAS ^{1}H NMR spectroscopy.[52,57-59] Essential amino acids such as phenylalanine, valine, lysine, tryptophan, and histidine and non-essential amino acids such as alanine, glutamate, tyrosine were detected in rat lenses.[52] After exposure to UV-B, a significant decrease was observed in the essential amino acids phenylalanine and valine, and in the non-essential amino acids glutamate and tyrosine.[52]

Glutamate is a non-essential free amino acid found in the lens and the aqueous humour.[60] It is largely converted from glutamine and is the most abundant excitatory neurotransmitter in the nervous system.[60,61] Glutamate penetrates poorly into the tissue, compared to other amino acids, and is utilized for production of CO_2, proteins and other metabolites.[60] Previous findings have shown that the epithelial cells of the lens have the highest rate of glutamate synthesis, and the fiber cells have low permeability of glutamate.[60] Thus, most of the glutamate metabolism takes place in the outer region of the lens. After exposure to UV-B radiation, whole-lens studies from rats showed a decrease in glutamate concentration.[52]

Metabolized amino acids

Hypo-taurine is a metabolic precursor to *taurine*. In vitro, hypo-taurine is a scavenger of some reactive oxygen species like hydroxyl radicals and singlet oxygen. In vivo, hypo-taurine is reported to quench oxidants, to function as an antioxidant and inhibit lipid peroxidation.[62] Specific oxidants such as singlet oxygen, hydroxyl radicals[63] and UV-R[64] might induce the oxidation of hypo-taurine to taurine. Taurine is known to be an osmolyte both in corneal and lens epithelial cells.[65,66] In human corneal epithelial cells, taurine is reported to enhance cell survival as a membrane stabilizer or as an antioxidant.[65] Taurine is suggested to protect the lens against oxidative stress and consequent cataract formation.[67] Both taurine and hypo-taurine are previously detected in extracts of rabbit cornea[54] and in intact tissue samples of the albino rat lens.[52]

Glucose metabolism, anaerobic metabolism

Lactate is formed when carbohydrates are used anaerobically for energy and is the major end product of lens glycolysis. The glucose metabolism in the lens is mainly anaerobic, and lactate is ultimately transported into the aqueous humour. Since lactate is an end product, it is often used as an indicator of the glycolytic pathway. In rat lens glycolysis, UV-B radiation is found to induce a reversible inhibition of glycolysis and also induce an accumulation of lactate inside the lens.[68] Löfgren and Söderberg have reported that after UV-B exposure to the albino rat a decrease in lens lactate dehydrogenase (LDH) activity was observed only in the anterior part of the lens.[69] LDH catalyzes the reduction of pyruvate to form lactate in carbohydrate metabolism. Risa et al. reported a decrease in lactate after UV-B exposure in the rat lens.[52]

Energy transfer

Energy metabolism is concerned with the reactions by which energy is made available to the organism. Like other cells, those of the lens need to have available chemical energy in the form of *ATP* (adenosine triphosphate) available for protein synthesis, active transport and synthesis of glutathione. The aerobic generation of ATP, the oxidative metabolism, is located in the lens epithelium and in the outer equatorial cortex. The fiber cells in the lens lack mitochondria and derive their energy mainly (90%) by glycolysis to lactate,[32] and the remainder entering the pentose phosphate pathway for synthesis of pentoses and NADPH.[32] The glycolysis to lactate is catalyzed

by lactate dehydrogenase (LDH) which is partially inhibited after exposure to UV-B radiation,[68] and this might lead to energy depletion in the lens. A reduction in ATP/ADP level is previously reported in Risa et al. after UV-B irradiation.[52,59]

Methyl donors and membrane building blocks

Choline is required for synthesis of phospholipids in cell membranes, methyl group metabolism and cholinergic neurotransmission.[70] Choline is absorbed by most tissues from foods containing choline and is either converted to betaine or is phosphorylated and used for synthesis of phospholipids (Fig. 7).[70] After UV-B exposure of rabbit corneas, choline concentration decreased substantially in a study performed by Sæther et al.[58] Previously, oxidative stress from photo-oxidation is found to affect choline transport into the lens and later phosphocholine synthesis.[71] *Phosphocholine* is formed by choline[71] (Fig. 7), and is among the organic phosphate compounds that decrease in concentration in some cataracts and in lenses that have been exposed to osmotic agents or oxidative stress.[72] After UV-B exposure of different doses, phosphocholine was found to significantly decrease in concentration in whole-lens rat studies.[52,59] *Betaine* is derived endogenously from the oxidation of choline and is an important methyl group donor to homocysteine to form methionine (Fig. 7).[70] Risa et al. have previously detected a decrease in betaine after exposure to UV-B radiation. [52,59]

Cell signalling / osmoregulation

The lens has a need to stabilize the intracellular osmotic pressure by regulating influx and efflux of water, osmolytes and other solutes. *Myo-inositol* is an important organic osmolyte in living cells and is one of the three major osmolytes in the lens besides sorbitol and taurine.[73] Influx of myo-inositol into the lens is dependent on the Na^+ dependent myo-inositol transporter (SMIT).[74] Previous studies have shown that high levels of myo-inositol in the mouse lens contribute to cataract formation.[75] In mice with hereditary cataract, a low level of myo-insitol was due to defect of the myo-inositol transport system and an enhanced efflux rate, and a dysfunction of the lens membrane was suggested.[76] In the whole-lens study performed by Risa et al., myo-inositol decreased significantly after UV-B exposure of rat eyes.[52] Another function of myo-

inositol is that of a cellular signal transducer and has a significant role in growth and differentiation.[77]

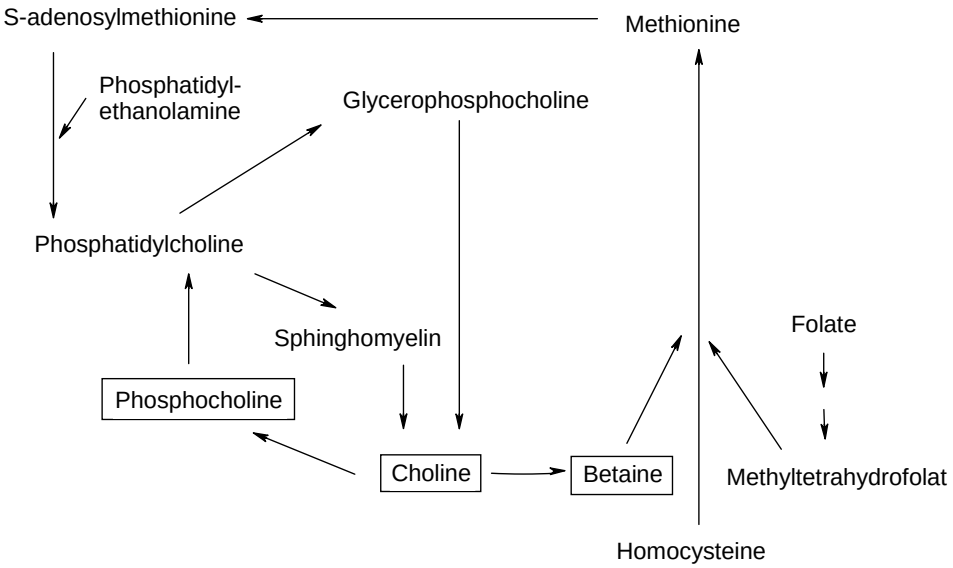

Figure 7. Metabolic pathways for choline and betaine (adapted from Zeisel et al.).[70] The formation of betaine from choline is irreversible. Betaine can donate a methyl group to homocysteine to form methionine. Methionine is converted to S-adenosylmethionine, an important methyl donor. Phosphocholine, phosphatidylcholine, glycerophosphocholine and sphinghomyelin are formed from choline and can be hydrolyzed to form choline. Phosphatidylcholine can be formed by sphingomyelin and phosphatidylethanolamine. Choline and folate metabolism is connected, because methyltetrahydrofolate is a product of folate metabolism and can also donate a methyl group for the formation of methionine from homocystein.

METHODS

Experimental animals

All the animals used for experiments in this thesis were kept and treated according to ARVO statement for the use of Animals in Ophthalmic and Vision Research. Adult albino rabbits (2.5-3.0 kg) were used in paper I and II, and six-week-old female outbred albino Sprague-Dawley rats (ca. 150 g) were used in the third paper of this thesis. The rabbit experiments were performed in the laboratory of our collaborators at the Institute of Experimental Medicine, Academy of Sciences of the Czech Republic, Prague. The rat experiments for the third paper were performed in the laboratory of our colleges in St. Eriks Eye Hospital, Karolinska Institutet, Stockholm, Sweden. The choice of species was made according to the species usually raised in the different laboratories of our collaborators.

UV-lamps

In paper I and II, the UV-A and UV-B source was portable UV lamps (366 nm and 312 nm wavelength, 6W, Bioblock Scientific, Illkirch, France). The radiant energy was measured with a radiometer (VLX-3W; Cole-Parmer, Vernon Hills, IL, USA) with a microprocessor equipped with two changeable sensors for UV-A and UV-B radiation.

In paper III, the UV-B source was a 350 W high-pressure mercury lamp (Oriel Instruments, Stratford, CT, USA) equipped with a water filter and a double monochromator. The water filter absorbs the infrared radiation and the double monochromator blocks stray light with improved contrast between wanted and unwanted wavebands. In the rat experiment in paper III, the monochromator was set for a maximum throughput at 300 nm and the entrance and output slits were adjusted to 10 nm full bandwidth at half maximum (FWHM). The irradiance at the corneal plane was measured with a thermopile, which measures the rise in temperature caused by the incident radiation. If the fused metal junctions of different types of metal (inside the thermopile) experience different temperatures, a voltage is generated between them and can be measured. The instrument was calibrated by the Swedish National Bureau of Standards. The wavelength distribution is shown in Figure 8. The maximum intensity was 300.1 nm, and the FWHM was 9.5 nm.

Exposure to UV-R

In paper I and paper II, the adult albino rabbits were anesthetized with 2% xylazine hydrochloride (0.2 ml/kg) and 5% ketamine hydrochloride (1.0 ml/kg), intramuscularly. The animals (n=11) were divided into three experimental groups, one serving as an untreated control group (n=3). Both eyes of four animals were exposed to UV-A irradiation and another four animals to UV-B irradiation. The total dose per day of UV-A radiation was 0.589 J/cm^2 and of UV-B radiation was 1.667 J/cm^2. The exposure time for both types of radiation was 8 minutes once a day in 5 days. The animals were sacrificed intravenously by thiopental natricum, 3 days after the last exposure day.

Before irradiation in paper III, the six-week-old female albino Sprague-Dawley rats (n=28) were anesthetized with a mixture of xylazine (11 mg/kg) and ketamine (80 mg/kg), intraperitoneally. To dilate the pupils, one drop of 0.5% of tropicamide was instilled in both eyes. One eye of each animal was exposed to UV-B irradiation (7 kJ/m^2) for 15 minutes, and the other eye served as a non-exposed control. One week after the UV-B exposure, the animals were killed by carbon dioxide asphyxiation.

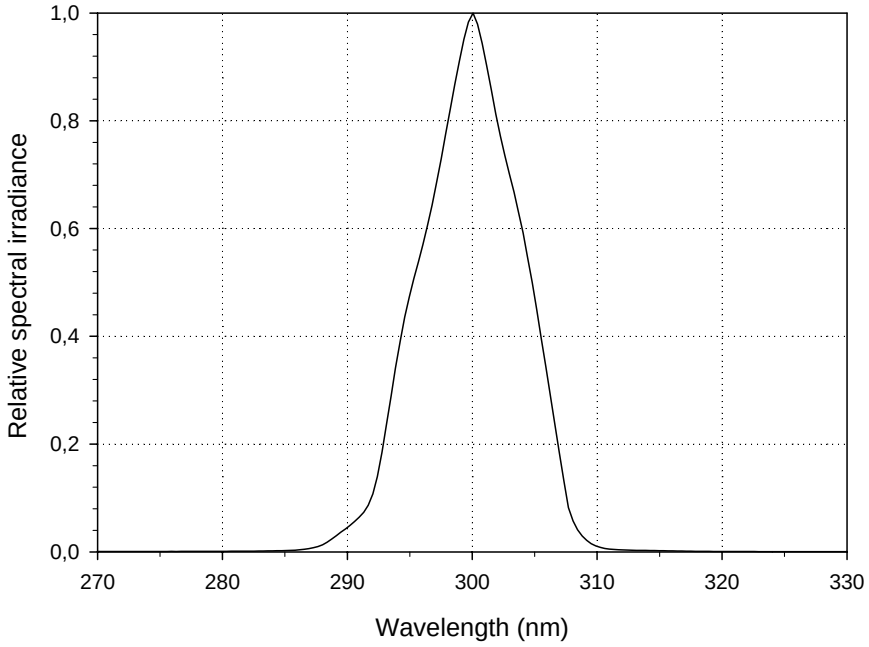

Figure 8. Spectral distribution of the radiation used in paper III

NMR spectroscopy

The basics of NMR

Nuclear magnetic resonance (NMR) spectroscopy is the use of magnetic properties of nuclei to study physical, chemical and biological properties of matter. The property of nuclear spins, which is characterised by the nuclear spin quantum number (*I),* is fundamental to the NMR phenomenon. The nuclei which possess *I*= ½ have two possible energy states (2*I*+1) and are the most suitable nuclei for NMR spectroscopy. Among the active nuclei in NMR spectroscopy, the ^{1}H nucleus has the highest sensitivity, the highest natural abundance (99.98%) and is present in almost all biological materials. Other isotopes such as ^{13}C, ^{31}P and ^{19}F are frequently used in NMR spectroscopy of biological material. Placed in a magnetic field, these nuclei are distributed by the Boltzmann distribution, where the lower energy level (α) contains slightly more nuclei than the higher level (β). By applying a radio frequent (RF) pulse to the nuclei, it is possible to induce transitions from the lower energy state to the higher energy state, perturbing the *Boltzmann distribution*. The energy distribution will return to equilibrium (Boltzmann distribution) by mechanisms of relaxation.

Relaxation and Fourier transformation

Relaxation is the general term for movements of spin systems towards equilibrium, and there are two major relaxation processes, *spin-lattice* (longitudinal) relaxation (T_1) and *spin-spin* (transverse) relaxation (T_2). T_1 is the time the spins use to return to equilibrium state from an excited state, and it depends on the type of nucleus, resonance frequency, mobility (viscosity) and presence of large molecules or paramagnetic ions. After a spin system has been excited by an RF pulse, it initially behaves like a coherent system where all microscopic components of the macroscopic magnetization precesses in phase (all together) around the direction of the external field. As time passes, these microscopic components start to lose phase coherence and this process is the T_2 relaxation time.

The relaxation is observable in NMR as the *free induction decay* (FID) and is important for the linewidth of a resonance. Fast T_2 relaxation results in broad peaks in the Fourier transformed spectrum. Slower relaxation rates produce longer FIDs and results in narrower resonances, which is preferable to facilitate the interpretation of

the NMR spectra (Fig. 9). To be able to interpret the FID, the oscillating signal must be separated into its components. With the use of the mathematical approach developed by Joseph Fourier (1768-1830) known as the *Fourier transformation*, it is possible to analyse the signal for its frequency components allowing for the intensity of each component to be measured. With today's computers, this operation is fast and takes only a few milliseconds.

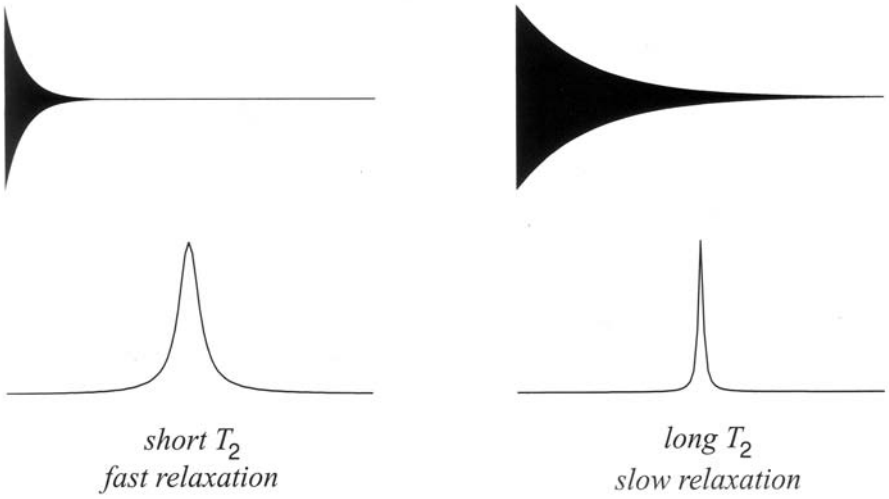

Figure 9. Fast decaying FIDs produce broad resonances, while slow relaxing FIDs produces narrower resonances (reprinted from Claridge: High-resolution NMR techniques in organic chemistry. 1999, with permission from Elsevier Ltd.).[78]

The use of NMR in medicine

NMR spectroscopy (in particular ^{1}H-NMR) is widely used to study metabolic composition in biological samples. ^{1}H-NMR spectroscopy has proved to be one of the most powerful technologies for examining biofluids such as urine and blood plasma,[79,80] and is the only existing technique capable of analysing metabolic composition of intact tissue. High-resolution (HR) ^{1}H magic angle spinning (MAS) permits direct analysis of excised intact tissues to obtain highly resolved spectra.

HR-MAS ^{1}H NMR spectroscopy

To obtain useful biochemical information from ^{1}H NMR measurements of tissues can be problematic due to line-broadening contribution to the NMR spectra. Biological tissues are semisolid complex structures containing macromolecules like proteins, lipids and low-weight metabolites. Due to the lack of molecular motion in biological tissues, line-broadening contribution is a problem by conventional solution-state NMR spectroscopy. The major line-broadening factors are a result of dipole-dipole interactions, chemical shift anisotropy and magnetic field inhomogeneities. The chemical shift anisotropies and dipolar couplings have an angular dependence of (3 $\cos^2$ θ-1), where 3 $\cos^2$ (54.7°)-1=0. Therefore, the development of HR-MAS solves the problem of line-broadening by averaging these factors to zero when spinning a sample at the magic angle of θ =54.7°, where θ is the angle between the sample spinning axis and the external magnetic field. The spinning rate is typically between 4000-5000 Hz. HR-MAS ^{1}H NMR spectroscopy has successfully been used in studies of biological tissues such as renal cortex and medulla[81], liver[82], heart,[83] brain,[84,85] breast,[86,87] cervical cancer [88], and recently on eye tissue.[52,57]

Even with the aid of the HR-MAS ^{1}H NMR technique, the resonances from biological tissue are still heavily overlapped. A challenge in the investigation of low-weight metabolites in biological tissues is the presence of proteins and other biological macromolecules, which cause broad lines that might mask the detection of small metabolites. These small metabolites can selectively be detected by relaxation editing since macromolecules generally have much faster T_2 relaxation times. One way to achieve such selectivity is to use the spin-echo Carr- Purcell-Meiboom-Gill (CPMG) sequence, acting as a T_2 filter suppressing signals from macromolecules with short T_2 relaxation times.[89] The CPMG sequence was used in all the HR-MAS experiments in this thesis for investigating tissues from cornea and lens.

Conventional solution-state NMR spectra can be obtained using extraction procedures for analysis of cells or tissues. These procedures are time-consuming and might be destructive for the metabolic composition of the samples due to the application of a strong acid (i.e. perchloric acid). Leaving an insoluble portion behind after extraction, metabolites may not be completely extracted and biochemical information may be

lost.[90] HR-MAS ^{1}H NMR does not suffer from any of these disadvantages. HR-MAS ^{1}H NMR spectroscopy is a fast and non-destructive technique which requires no sample pre-treatment and need only small sample volumes for the metabolic analysis.

Quantitative 1D NMR spectroscopy is a powerful tool to determine absolute concentrations because of the direct proportionality of signal intensity to the quantity of analyte present in the sample. It is widely used in many fields of chemistry, biology and medicine. A major drawback is the difficulty of calibrating the spectra with sufficient accuracy. In vitro, a reference compound is often added to the sample, the so-called internal standard. The choice of a reference compound is difficult because there should be no chemical interaction with the sample, the reference compound should have a chemical shift separated from the shifts of the compounds in the sample and have no co-solubility with the sample. This has until now been a drawback using HR-MAS on intact tissue, and concentrations relative to control-material has been used in our analysis.[57]

Interpretation and assignment of NMR spectra

Peak assignments of the NMR spectra in this thesis were performed according to previous reports.[52-54,91,92] A large amount of peaks and spectral overlap made the use of two dimensional (2D) NMR techniques useful. Common methods as homonuclear correlated spectroscopy (^{1}H-^{1}H-COSY) and J-resolved spectroscopy (JRES) were recorded in order to assign complicated coupling patterns. For identification of some peaks in the ^{1}H HR-MAS spectra, inverse detected ^{1}H-^{13}C spectroscopy was applied.

NMR-based Metabonomics

Metabonomics is defined as "the quantitative measurement of the time-related multiparametric metabolic response of living systems to pathophysiological stimuli or genetic modification".[93] This concept has arisen from the application of ^{1}H NMR spectroscopy to study metabolic composition of biofluids and tissues by using pattern recognition (PR) methods to interpret complex NMR-generated data sets. The complexity and the presence of natural biological variation make it difficult to extract all the available information from a NMR spectrum. Data reduction and PR methods is shown to be appropriate for accessing this latent biochemical information from the

NMR spectra. Combining these multivariate statistical methods and NMR spectroscopy is currently the only effective way to extract meaningful metabonomic information from biofluids and tissues.[94]

High-resolution ^{1}H NMR spectroscopy coupled with principal component analysis (PCA) is a well-established technique for studying the endogenous metabolic changes in biofluids such as blood and urine, caused by drug toxicity or disease processes. Different pathological stimuli (e.g. UV-R) can produce characteristic changes in the concentration and pattern of metabolites. Such studies can provide information about the site of pathology, the basic mechanism(s) and potential biomarkers of specific pathology.[95]

Principal Component Analysis (PCA)

One of the most useful and easily applied pattern recognition methods is PCA. PCA is a projection method that visualizes important information hidden in a complex data set, and finds if one sample is different from another and if variables are correlated or not. New uncorrelated variables, *principal component*s (PCs), are created from a linear combination of the original variables with appropriate weighting coefficients. The first principal component (PC1) is oriented along the direction of maximum variance in the data set. The second principal component (PC2) will orient along a direction that is orthogonal to the first PC and in the direction of the second largest variance, and so on. The projections of the samples (individual NMR spectra) are defined as scores, revealing the relationship between the samples. A plot (score plot) of the first two or three PCs gives the "best" information content of the data set in two or three dimensions. This plot can visualize clustering behaviour on metabolic response to a pathophysiological stimulus (i.e. exposure to UV radiation to the eye). Another graphic representation important for the interpretation of the PCA is the loading profile, which displays the importance of each variable/metabolite for the variation described by the different PCs. The plot describes how much the variable/metabolite contributed to the PC and how well that PC takes the variation of that variable into account over the data points. The score plot from the PCA is used in all three papers presented in this thesis.

Validation of a model is important to establish how well it will perform for future samples. To validate a model is searching for the number of PCs where all variation is described and where no noise is modelled. All validation should be performed by the use of a separate test set, including the same type of samples as the calibration set. In practice, this indicates a double amount of samples as the calibration set. When samples are too expensive or when laboratory animals or human material are used for analysis, a possible, and acceptable, solution is to use cross validation. To use full cross validation implies that the same samples are used both for model estimation (calibration) and testing (validation). The basis of cross validation is that one sample is kept out when the model is calibrated on the rest of the samples. Values are predicted for the left-out sample and prediction residuals are calculated. The process is repeated until all samples have been kept out once and then all prediction residuals are combined to find the overall root mean square error of prediction.

Soft Independent Modelling of Class Anology (SIMCA)

SIMCA is a supervised pattern recognition method where the aim is to predict if samples (NMR spectra) belong to potential classes. All samples are predefined in advance to belong to a separate class, and the SIMCA method will detect if these samples belong to a single class, to multiple classes or to no class. When focusing on the similarities between the members of the same class, a statistical measure on the differences between the samples can be obtained. To visualize the class membership of the samples, the Coman´s plot or "*si vs. si*" plot (Si = object-to-model distance) shows the sample-to-model distances plotted against each other for two models. It includes class membership limits for both models, making it possible to see whether a sample is likely to belong to one class, or both, or none.

The SIMCA method is based on separate PCA models performed on the predefined classes, making up a training set. This training set is used to describe each class by the model defined by the principal components, and the classification of samples can be performed by implementation of F-tests to test for significance. Because every class has to support a PCA model, classification is only applicable with several samples in each class.

Additional statistics

In order to compare individual resonances from the NMR spectra of exposed eye tissue (cornea and lens) to non-exposed eye tissue, the absolute peak integrals of selected resonances were measured and normalised by the sample wet weight both in paper II and III. The peak integrals in the UV-R exposed eye tissue were presented relative to the peak integrals in the non-exposed eye tissue. The difficulty of finding a reference compound without any chemical interaction with the sample tissue, did not allow for measuring absolute concentrations of the single metabolites in the eye tissue. The normalised peak integrals were used to obtain a statistical measure of changes in single metabolites after UV-R exposure. After normality tests were approved, t-tests and one-way ANOVA followed by Bonferroni (multiple comparison test) were performed between exposed and control material in this thesis. In all papers, the level of significance was set to $p<0.05$, and the confidence level was set to 95%.

OBJECTIVES

The objectives of this thesis were to:

1. Identify metabolic differences between the effects of UV-A and UV-B irradiation on the metabolic profiles of rabbit aqueous humour, cornea and lens (paper I, II).
2. Utilize HR-MAS ^{1}H NMR, a non-destructive method, on intact tissue from cornea and lens. (paper II, III).
3. Introduce NMR-based metabonomics to aqueous humour, cornea and lens (paper I, II, and III).
4. Investigate metabolic changes in different compartments of the rat lens after exposure to a high dose of UV-B radiation (paper III).

SUMMARY OF PAPERS

Paper I

Tessem MB, Bathen TF, Čejková J, Midelfart A. Effect of UV-A and UV-B irradiation on the metabolic profile of aqueous humor in rabbits analyzed by ^{1}H NMR spectroscopy. *Invest Ophthalmol Vis Sci*. 2005;46:776-781.

Aqueous humour from rabbit eyes exposed to UV-A (366 nm, 0.589 J/cm^2) or UV-B irradiation (312 nm, 1.667 J/cm^2) was analysed by ^{1}H NMR spectroscopy and principal component analysis (PCA). The present study was the first to use NMR-based metabonomics on aqueous humour, interpreting changes induced by pathophysiological stimuli to the eye. PCA visualized the pattern of metabolic differences between the normal and the UV-B exposed aqueous humour. UV-B irradiation caused statistically significant alterations of the metabolites; betaine, glucose, ascorbate, valine, isoleucine and formate in the rabbit aqueous humour. These metabolic alterations after UV-B irradiation suggest several effects in the eye such as permeability and osmoregulatory problems (betaine, glucose, valine, isoleucine), oxidation (ascorbate, formate) and deactivation of glycolytic enzymes (glucose). The PCA visualized no separation between the normal and the UV-A irradiated samples of aqueous humour and no significant metabolic changes were detected. The study showed that ultraviolet rays with shorter wavelengths (UV-B) had larger influence than rays with longer wavelengths (UV-A) on the metabolic profile of rabbit aqueous humour. The focus on the metabolic profile of aqueous humour seems to be important in understanding the complete biochemical processes in the development of UV-R cataract. This is especially interesting with respect to the known UV-filtering effect of aqueous humour protecting against pathogenesis of cataract.

Paper II

Tessem MB, Bathen TF, Čejková J, Midelfart A. Effect of UV-A and UV-B irradiation on the metabolic profile of rabbit cornea and lens analysed by HR-MAS ^{1}H NMR spectroscopy. *Ophthalmic Res*. 2006;38:105-114. (Published online Desember 22, 2005)

Intact tissue of rabbit cornea and lens from eyes exposed to UV-A (366 nm, 0.589 J/cm^2) or UV-B irradiation (312 nm, 1.667 J/cm^2) was analysed by HR-MAS ^{1}H NMR spectroscopy and pattern recognition methods (PCA and SIMCA). Rabbit

cornea exposed to UV-B irradiation showed metabolic profiles significantly different from the normal metabolic profiles of cornea, and a significant decrease was found in metabolites such as ascorbate (84%), myo-inositol (59%), hypo-taurine (91%) and choline (76%). These observed metabolic alterations in the cornea might be explained by oxidation (ascorbate, hypo-taurine), osmoregulation (myo-inositol, hypo-taurine and choline), disturbance of membrane function and cell transport (choline, myo-inositol). Exposure to UV-A radiation caused no significant metabolic changes in the cornea. The metabolic profiles of the rabbit lenses showed no significant metabolic changes after repetitive UV-A or after repetitive UV-B irradiation. UV-B absorption by the corneal tissue seems to be of protective character to the biochemistry of the rabbit lens tissue.

Paper III

Tessem MB. Bathen TF, Löfgren S, Sæther O, Mody V, Meyer L, Dong X. Söderberg PG, Midelfart A. Biochemical response in various compartments of the rat lens after in vivo exposure to UVR-B analyzed by HR-MAS ^{1}H NMR spectroscopy.

Different lens compartments (anterior, posterior, nucleus and equator) from rat eyes exposed to acute double threshold dose UV-B radiation were analysed by HR-MAS ^{1}H NMR spectroscopy followed by principal component analysis. The scores from the PCA showed that samples from the UV-B exposed lenses were different from the contralateral non-exposed lenses. Metabolic changes were observed in GSH, phosphocholine, myo-inositol, succinate, formate, ATP/ADP and in the amino acids phenylalanine, taurine, hypo-taurine, tyrosine, alanine, valine, isoleucine and glutamate. The score plot from the PCA showed separation of the metabolic profiles between all the lens compartments, except between the anterior and the posterior part which were distributed without any clear pattern. This was true both in exposed and in non-exposed lenses. The most substantial metabolic changes after UV-B exposure were found in the anterior part of the lens, while the nucleus showed the smallest changes. The variation in compound concentrations among the lens compartments became smaller after UV-B exposure. GSH and ATP/ADP were the only compounds with a lower concentration in the nucleus than in the anterior part after exposure to UV-B. This was true for 12 out of 16 compounds in the contralateral non-exposed lenses. The present study shows the importance of analyzing biochemistry in distinct compartments of the lens.

RESULTS AND DISCUSSION

Biochemical responses in the anterior part of the eye after exposure to UV-R

^{1}H NMR spectroscopy provided metabolic profiles of aqueous humour from rabbit eyes exposed to UV-A and UV-B radiation, detecting 23 different metabolites (paper I). The metabolic profiles of rabbit corneas and lenses exposed to in vivo UV-A and UV-B radiation were obtained by HR-MAS ^{1}H NMR spectroscopy (paper II). Respectively, 16 and 20 different metabolites were observed in the cornea and the lens. In paper III, 26 different metabolites were detected by HR-MAS ^{1}H NMR spectroscopy in the different compartments of the albino rat lens after exposure to in vivo UV-B radiation. A large amount of metabolic information was extracted from the NMR spectra in all papers.

To interpret these complex data sets, the use of NMR-based metabonomics was found useful to extract valuable information about metabolic changes after exposure to UV-R. PCA was effective in confirming differences in the metabolic profiles after irradiation. In rabbit aqueous humour and corneas, PCA showed that the metabolic profiles after in vivo UV-B radiation were different from the controls. In the rabbit lens (paper II), there was no difference observed between the metabolic profiles of UV-B exposed and control animals. In the albino rat eyes (paper III), differences in metabolic profiles were observed between the lens compartments from UV-B exposed eyes and from the contralateral unexposed eye. Differences were also found between profiles of different compartments within exposed and within unexposed lens regions. After in vivo UV-A irradiation (paper I and II), there was no difference in the metabolic profile in the rabbit aqueous humour (paper I), cornea or lens (paper II).

The results obtained from the use of NMR-based metabonomics made a further investigation of each metabolite in the metabolic profiles interesting. By quantifying compounds in the exposed material relative to compounds in the unexposed material, changes in separate metabolites could be measured. A summary of the results

Table 1. Summary of results obtained after in vivo UV-R exposure to the anterior eye of rabbits and rats (significant changes are presented with bold numbers)

Detected compounds grouped by function	**Metabolic alteration after in vivo UV-B exposure (%)**							
	Rabbit (paper I)		***Rabbit (paper II)***		***Rat (paper III)***			
	Aqueous humour		**Cornea**		**Lenses (UV-B)**			
	UV-A	UV-B	UV-A	UV-B	**Ant.**	**Nucl.**	**Post.**	**Eq.**
Antioxidants								
Glutathione					**-40**	-13	+11	-18
Ascorbate	-21	**-64**	-20	**-84**				
Amino acids								
Essential								
Isoleucine	+36	**+168**	-13	-8	**-60**	**-46**	**-57**	**-53**
Valine	+4	**+83**	-8	+4	**-60**	**-48**	**-59**	**-66**
Histidine	-2	+28						
Phenylalanine					**-68**	**-53**	**-58**	**-69**
Non essential								
Tyrosine					**-71**	**-56**	**-56**	**-70**
Alanine	+20	+13	-4	-26	-24	**+23**	+19	+17
Glutamate					**-32**	-7	-10	-24
Metabolized amino acids								
Taurine			-21	-44	**-58**	**-35**	**-36**	**-41**
Hypo-taurine			-15	**-91**	**-61**	**-39**	**-45**	**-52**
Glucose metabolism								
Glucose	+31	**+73**	-2	+107				
Pyruvate	+123	+24						
Anaerobic metabolism								
Lactate	+2	+21	-12	-2	-16	**+21**	+5	-8
Aerobic metabolism								
Succinate					**-38**	+0.5	-9	**-36**
Citrate	+6	-15						
Acetate			+1	-4				
Energy transfer								
ATP/ADP					**-49**	-13	+17	-12
Metabolic end product								
Formate	+7	**+114**			**-40**	-11	**+20**	-8
Methyl group donors								
Betaine	+130	**+592**	+20	**+148**				
Choline			-1	**-76**				
Membrane building block								
Phosphocholine					**-43**	**-16**	**-20**	**-31**
Cell signalling								
Myo-inositol			+8	**-59**	**-67**	**-53**	**-54**	**-58**

obtained after exposure to in vivo UV-R to the anterior part of the eye is presented in table 1.

Antioxidants

In agreement with previous findings using ^{1}H NMR spectroscopy,[53,55] *ascorbate* was detected in the aqueous humour (paper I) and in the cornea from rabbits (paper II). Ascorbate was not observed in the rabbit lenses (paper II) and the rat lenses (paper III), which is consistent with previous analysis performed both with HR-MAS ^{1}H NMR spectroscopy[52,57] and with ^{1}H NMR spectroscopy of tissue extracts.[53,92] In aqueous humour and in cornea from rabbits (paper I and II), a significant decrease in ascorbate concentration was observed after UV-B exposure (Tab. 1). The corneal reduction of ascorbate is consistent with a previous analysis in our laboratory performed on rabbits by Sæther et al.[58] The reduction of ascorbate is probably due to the mechanisms described by Ringvold,[40,50] where the aqueous humour and the cornea function as UV-R filters, protecting the lens and retina by mechanisms such as absorption, fluorescence-mediated ray transformation and fluorescence reduction.[40,50] After UV-A exposure to the rabbit eye, a reduction of ascorbate was observed, but the change was not statistically significant. Ascorbate is however found to have the highest UV-R absorption between wavelengths of 280 and 310 nm.

The vital lens antioxidant, *glutathione* (GSH) was observed in the HR-MAS NMR spectra in both rabbit lenses (paper II) and in rat lenses (paper III). GSH was not detected in rabbit cornea (paper II) or aqueous humour (paper I). This is in agreement with previous findings from our laboratory.[54,92] A 40% decrease in GSH concentration after exposure to an acute double threshold dose of UV-B was observed only in the anterior part of albino rat lenses. The other parts of the lens remained unchanged. The high GSH concentration in the anterior part of the lens might reflect protection of cell proliferation and lens fiber elongation against oxidation. A very low concentration of nuclear GSH was found in paper III and is in consistence with previous studies of normal lenses.[51] However, if the decrease in GSH was due to oxidation, the oxidized glutathione (GSSG) should be observed in the NMR spetra. The problem is that GSH and GSSG have almost the same resonances in the HR-MAS ^{1}H NMR spectra. There is however a difference in β-CH_2 of cystein where the resonance of GSH (Cys.2) is

4.57 ppm and the GSSG resonance is at 4.77 ppm. In paper II and paper III, it was not possible to assign GSSG in the lens ^{1}H NMR spectra. In a few spectra there might be a trace of signal in this region, but the signal to noise region was very low and the assignment of GSSG was not possible. The same lack of GSSG resonances was experienced also in previous studies from our laboratory, using HR-MAS ^{1}H NMR.[52,57] An explanation to this might be that the oxidation process mainly produces protein-linked GSSG, which is difficult to observe with this method. This is because the CPMG spin echo sequence will suppress the signals from macromolecules such as proteins.[89]

Amino acids

Valine and isoleucine were assigned in all the compartments of the anterior part of the eye, confirming previous studies using ^{1}H NMR spectroscopy.[52-55] In rabbit aqueous humour (paper I), the essential amino acids *valine* and *isoleucine* were significantly increased after exposure to UV-B radiation. Exposure to UV-A radiation caused no significant change in these amino acids. The increase of valine and isoleucine in aqueous humour might indicate impaired protein synthesis. After UV-B exposure of the rat eyes, a substantial decrease of valine (48-66%) and isoleucine (46-60%) was found in all the lens parts (paper III) (Tab. 1). This might indicate that UV-B exposure causes problems with transport or permeability between the lens and the aqueous humour.

Glutamate was in the present thesis assigned in NMR spectra from rabbit lenses (paper II) and in different parts of rat lenses (paper III). This confirms previous findings from our laboratory.[53,92] In the rabbit aqueous humour (paper I), glutamate was not assigned. After in vivo UV-B exposure to the rats (paper III), a 32% decrease was observed in the anterior region of the lens. In the other compartments of the lens, the level of glutamate remained unchanged. This is in agreement with other studies showing that the epithelial cells have the highest rate of glutamate synthesis.[60] Previous whole-lens studies from rats in our laboratory showed that the glutamate concentration was not changed after exposed to a similar dose of UV-B radiation.[52] This result illustrates the importance of analyzing biochemistry of the lens in separate compartments.

Tyrosine is an amino acid suggested to be a hydroxyl radical scavenger, singlet oxygen quencher and a weak photo sensitizer.[48] However little is known about tyrosine in the eye. Similar to previous results with ^{1}H NMR spectroscopy,[53,55] tyrosine was detected in the rabbit aqueous humour, in the rabbit lens and in the rat lens in the present thesis. A decrease of 56-71% was detected in all rat lens compartments after UV-B exposure (Tab. 1). This decrease might be a result of the suggested functions as a radical scavenger, oxygen quencher and a photosensitizer. [48]

Phenylalanine is an essential amino acid and is closely related to tyrosine, which has an additional hydroxyl (OH) group. An enzyme called phenylalanine hydroxylase can convert phenylalanine to tyrosine by hydroxylation. (Fig. 10). An alteration in concentration level of phenylalanine might therefore affect the concentration of tyrosine. Phenylalanine was in the present thesis assigned in the rabbit aqueous humour and in the different compartments of the rat lenses, which is consistent with previous studies.[52,55] In the rat lens, phenylalanine was quantified and showed that the concentration level decreased by 53-69% after exposure to UV-B radiation (Tab. 1). This decrese might explain the decrease in concentration of tyrosine (Fig. 7). UV irradiation is previously reported to cause formation of *alanine* from phenylalanine in the presence of hydrogen peroxide.[96] The present increased level of alanine in the nucleus might be a result of this degradation. An increased level of alanine after UV-B exposure was in agreement with whole-lens studies by Risa et al.[52,59]

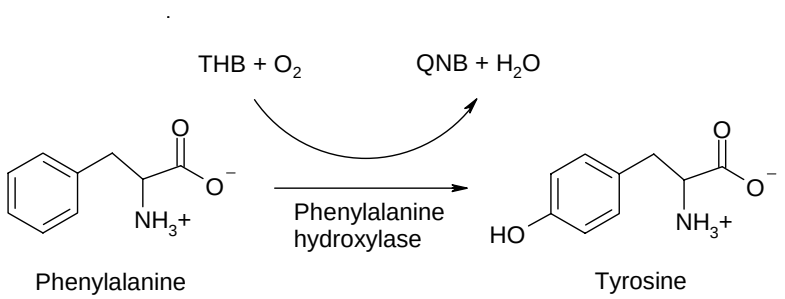

Figure 10. Degradation of phenylalanine to tyrosine. Tetrahydrobiopterin (THB) is reduced to Quinonoid dihydrobiopterin (QNB) (adapted from Stryer).[97]

Metabolized amino acids

Hypo-taurine has previously been discussed as the metabolite with the most excessive decreases in the lens after UV-B exposure.[52] Similar to previous reports,[52,54,55,92] hypo-taurine was not detected in the rabbit aqueous humour (paper I), but was observed in rabbit corneas (paper II), rabbit lenses and rat lenses (paper III). In the rabbit corneas, exposure to UV-B radiation caused almost complete depletion (91% decrease) of hypo-taurine. This substantial decrease in the rabbit cornea might be a result of the radical scavenging and antioxidant functions. The same mechanism might be acting in the rat lenses when hypo-taurine decreased by 52-61% (Tab. 1) in the different lens compartments after exposure to UV-B radiation (paper III). An inhibition of lipid peroxidation might also be a function of hypo-taurine in rabbit cornea and rat lenses exposed to UV-B radiation.

UV-R is reported to induce the oxidation of hypo-taurine to *taurine*[64] and this might cause the decrease of hypo-taurine both in rabbit cornea and in rat lenses (paper II and III). However, UV-B exposure caused a decrease (40%) in taurine in the rabbit corneas and a decrease (41-58%) in the rat lenses (paper III) (Tab. 1). This decrease observed in both rabbit cornea and in rat lens regions after UV-B exposure might be associated with the suggested osmotic, antioxidant and membrane functions of taurine. The results are in consistence with the whole-lens rat study performed by Risa et al.[52]

Glucose metabolism

Glucose from the aqueous humour is the main source of energy in the metabolism of the cornea and the lens. Glucose was assigned both in the rabbit aqueous humour and in the rabbit corneas, similar to previous studies in our laboratory.[54,55] In the rabbit aqueous humour, the glucose concentration increased by 73% after exposure to UV-B radiation. Previous studies performed by Hightower and McCready[18] on cultured rabbit lenses, showed that the initial effect of UV-B radiation was impaired permeability and transport problems in the lens membrane, affecting the glucose transport. In addition, impairment of glycolytic enzymes after UV-B exposure might impair glycolysis[18,25,68] and thereby contribute to an elevation of glucose in aqueous humour. Inflammatory responses after UV-B exposure might induce impairment in blood-aqueous barrier and can explain the glucose increase in the aqueous humour.

Plasma contains a higher concentration of glucose than aqueous humour[98] and leakage from the plasma will increase the aqueous level of glucose.

Aerobic and anerobic metabolism

Succinyl-CoA synthetase is a mitochondrial enzyme of the Krebs cycle that catalyzes the conversion of succinyl-CoA into *succinate*. Simultaneously, 1 molecule of GTP (guanosine triphosphate) is formed from GDP (guanosine diphosphate) and inorganic phosphate, and 1 molecule of co-enzyme is regenerated. Succinate dehydrogenase is a membrane bound enzyme which converts succinate to fumarate as part of the Krebs cycle. Succinate was assigned in the rabbit aqueous humour (paper I), and in the different regions of the albino rat lenses (paper III). After exposure to UV-B, succinate decreased in the anterior (38%) and the equatorial part (36%) of the rat lens. The irradiation might have a negative effect on the enzyme (Succinyl-CoA) which produces succinate in the Krebs cycle. A decrease in succinate concentration was also found in Risa et al. after UV-B exposure.[52,59] In the nucleus and the posterior parts of the albino rat lenses (paper III), the concentration of succinate remained unchanged. This is most likely explained by the lens epithelium, being the main centre of aerobic metabolism. In the nucleus, *lactate* concentration was increased by 21% and probably due to increased anaerobic glycolysis, catalyzed by lactate dehydrogenase (LDH).

Metabolic end product

The end metabolite *formate* was detected in rabbit aqueous humour, in rabbit lenses (paper I, II) and in all the different compartments of the rat lenses (paper III). In the rabbit aqueous humour, the concentration increased significantly by 114% after UV-B exposure. In the anterior region of the albino rat lenses, formate decreased by 40%, but increased by 20% in the posterior lens region (paper III). Formate is a metabolite with a rather unknown importance in the eye, but has previously been detected by ^{1}H NMR spectroscopy in extracts of cornea and lens[53,54] and in samples of aqueous humour.[55] A possible source of formate in mammalian systems may be formaldehyde, which is rapidly oxidized to formate.[99] Formate is incorporated into synthesis of folic acid where the enzyme cobalamin (vitamin B_{12}) is included. An inactivation of cobalamine is previously found to cause accumulation of formate.[100] The use of cobalamin in combination with other vitamins (B_3 and B_9) was found to protect against damaging effects of UV radiation.[101] The increase of formate in the rabbit aqueous humour may have a relation to the damaging effects of UV-R on these

vitamins. However, formate is reported to have other functions and effects such as inhibiting cytochrome oxidase activity, being a component involved in ATP synthesis[102] and to be a toxic metabolite.[103]

Energy transfer

Adenosine triphosphate/diphosphate (ATP/ADP) was detected in both the rabbit lenses in paper II and in the rat lenses in paper III. A 41% reduction of these high-energetic phosphates was found in the anterior part of the albino rat lens after exposure to UV-B radiation (paper III). The other lens regions showed no significant change in ATP/ADP concentration after UV-B exposure. The glycolysis to lactate is suggested to be reduced because lactate dehydrogenase is found to be inhibited by exposure to UV-B radiation in the rat lens.[68] However, the lactate concentration was not changed in the anterior part of the rat lens after UV-B exposure (paper III). An explanation might be the high energy requirement of GSH turnover in the lens.[104] UV-B exposure caused a 40% decrease in GSH in the anterior region of the rat lens (paper III), and might explain the reduction of ATP/ADP. A previous study showed that synthesis of phosphocholine parallels a decrease in ATP concentration,[72] and in general, repair processes after photochemical damage require increased amount of energy.[105]

Methyl donors

Choline was detected in the rabbit cornea and in the rabbit lens (paper II) and in the different compartments of the rat lens (paper III). In the rabbit corneal tissue, the choline concentration decreased by 76% after exposure to UV-B radiation, which is consistent with previous ^{1}H HR-MAS study by Sæther et al.[58] In rabbit aqueous humour (paper I), choline was not assigned, but the concentration of *betaine* increased substantially (Tab. 1). UV-B radiation is as previously described able to disrupt cell membranes[18] and cause apoptosis in corneal tissue.[35] Membrane damage after UV-B exposure might have caused a leakage of choline into the aqueous humour where oxidation to betaine has occurred (Fig. 7). Another suggestion might be an impaired transport of choline into the corneal tissue. The suggested functions of betaine are as an osmolyte[70] and as a stabilizer of macromolecules.[106] Choline was not quantified in the rat lenses.

Membrane building block

Phosphocholine was assigned only in the different compartments of the rat lenses in paper III. In vivo UV exposure caused a 16-43% decrease in phosphocholine where the largest decrease was observed in the anterior region (Tab. 1). This was in agreement with the whole-lens rat studies by Risa et al.[52,59] UV-B exposure might have affected choline transport into the lens and thereafter synthesis of phosphocholine, as suggested by Jernigan et al.[71] Previous studies found that a decrease in synthesis of phosphocholine paralleled a decrease in ATP, which is in agreement with paper III. Further, an increased efflux of phosphocholine was previously detected in lenses subjected to oxidative stress.[72] This might explain the decrease in phosphocholine in the rat lenses.

Cell signalling /osmoregulation

Myo-inositol was observed in the rabbit aqueous humour, cornea and lens (paper I and II) and in all the different regions of the rat lens (paper III). This was in agreement with previous reports from our laboratory.[52,55,57,58] In the rabbit cornea (paper II), myo-inositol decreased by 59% after exposure to UV-B radiation. UV-B has previously been found to cause membrane disruption[18] and apoptosis[35] in corneal tissue. Both these mechanisms might explain the decrease of myo-inositol found in the rabbit cornea. In the different lens compartments from albino rats (paper III), the concentration of myo-inositol decreased by 53-67% (Tab. 1). This is in agreement with the results from Risa et al. on whole-lens studies after in vivo UV-B exposure.[52] The UV-B radiation might disturb the osmotic function,[66] the cellular signalling function, and the function myo-inositol have on cellular growth and differentiation.[77]

Experimental design

UV-R dose

The daily UV-B doses (1.667 J/cm^2) used in paper I and paper II are reported to be close to threshold values for developing permanent cataract after a single application on pigmented rabbit eyes.[16] For the cornea, the daily UV-B dose was higher than the threshold dose for permanent damage in pigmented rabbits.[16] The exposure time and the experimental condition were the same for both UV-B and UV-A radiation. With this experimental set-up, the daily dose of UV-A (0.589 J/cm^2) was lower than the UV-B dose. The applied single UV-A dose in paper I and II was lower than previous

reported threshold values.[16] The cumulative effect of repeated exposures for 5 days must be taken into account when evaluating the effect of UV-R exposure on the metabolic profiles in paper I and II. Due to design differences, it is difficult to make comparisons with previous studies. According to a report by Zigman,[107] the daily UV-B dose applied in paper I and II is roughly equivalent to exposing the human cornea to approximately 16 hours of sunlight, whereas the daily UV-A dose is equivalent to approximately 10 minutes of sunlight.

The UV-B dose used in paper III (7.5 kJ/m^2) is above threshold for permanent lenticular damage in the rat.[108] The dose-response relationship between in vivo UV-B irradiation and lens opacities in rats has previously been quantified.[108] The intensity of forward light scattering in the lens of the albino rat increases exponentially with increased UV-R dose between 0.1 and 14 kJ/m^2.[108] The forward light scattering for the present dose (7.5 kJ/m^2) increases to 140% of that in the unexposed lenses. The observation of the anterior cortical lens opacities in paper III is in agreement with those reports. The high dose of UV-B used in this study was chosen for comparison with the previous whole-lens studies by Risa et al.[52,59]

The optimal point of time for metabolic analysis in the anterior eye after UV-R exposure

Different points of time for metabolic analysis were used in the two first papers compared to paper III. In the two first papers, rabbits were killed three days after the last exposure day, but the rats in paper III were killed one week after irradiation. In a pilot study performed by our collaborators at the Institute of Experimental Medicine, Academy of Sciences of the Czech Republic, Prague (unpublished), accumulation of metabolic changes in the rabbit cornea could be detected 3 days after irradiation, and therefore, the rabbits in paper I and II were sacrificed 3 days after the last exposure day. Extensive research from the Swedish group on maximum light scattering of the rat lens, found it optimal to detect close-to-threshold UV-R-induced cataract one week after exposure.[109] Most of their studies are based on this optimal time of one week after in vivo irradiation.[110-112] A time-dependency study of metabolic changes in rat lenses after UV-B irradiation was recently carried out in our laboratory.[59] The metabolic response seemed to be delayed compared to the detection of light scattering

in the lens. These studies were performed on rats, and in rabbits the optimal time of observation might be different. To asses the most suitable design for studying the progress and recovery in cornea and lens metabolism after UV-R exposure, further studies are needed.

Control animals or contralateral eye as unexposed?

In paper I and II, both eyes of each rabbit were irradiated with UV-A or UV-B, and both eyes of animals without treatment were used as controls. Individual control animals were used to assure that the control samples were not affected in any way by the irradiation. The intraocular influence has been discussed before, particularly regarding the general reaction in the body towards the eye damage. A study by Diestelhorst and Krieglstein (1991) revealed a significant increase in aqueous humour flow by 14% after trabeculectomy (a surgical procedure that removes part of the trabeculum in the eye to relieve pressure caused by glaucoma), and concluded that this response was mediated by the central nervous system.[113] Another study performed after trabeculectomy demonstrated that the fellow eye does not behave absolutely in the same manner, making intra individual comparisons not feasible.[114] On the basis of this discussion, control animals were found to be the appropriate approach for the rabbit experiments in the first two papers.

In paper III in this thesis, the rat experiments were performed with the contralateral eye as the non-exposed reference. This method avoids all individual variation between exposed and unexposed material. For analysis of the cornea and the lens, this might be the correct approach, but the subject is still disputed and the correct design might be discussed further. The reason for the different design in the studies of the present thesis is the different protocols used in the collaborating laboratories.

Animal species, pigmented or albino animals?

The most commonly used species for in vivo experiments are probably rabbits, rats and mice, and all these species have frequently been used in UV-R cataract research. The human eye is in many respects different from both the rabbit and the rat eye, which is used in this thesis. Most important for the present studies are the dimensions of cornea and lens. The human cornea (520-550 μm) is about five times thicker than the rat cornea (120-160 μm) and therefore transmits less UV-R.[15] The rabbit cornea

(380-400 μm) is thicker than the rat lens and closer to the human thickness.[15] The rat and rabbit lenses are in addition not as flat as the human lens. However, the general structure, growth pattern and the proteins in rats and rabbits are found to be comparable to the human lens.[26]

Albino rabbits and rats were used in the present studies. Pigmented species would be more similar to human eyes than albino eyes and would probably be a better choice for comparison studies. The ground squirrel has been proposed as a good model because it is melanin pigmented and diurnal. Rabbits and rats are nocturnal animals and have less amount of ascorbate in the anterior segment than the diurnal animals.[115] Unfortunately, only albino species were available in the collaborating laboratories and available from commercial breeders at the time of performance.

Topography of lens metabolism

The comparison of the nucleus and the cortical region of the rabbit lens after both UV-A and UV-B exposure showed no spectral differences by the PCA (paper II). Prior to NMR analysis, the division of the tissue might not have been accurate enough for this purpose. Thus, each sample might include fragments of tissues from both the cortex and nucleus, and might therefore explain why metabolic difference between the nucleus and the cortex of the rabbit lens was not detected. An improvement of the slicing technique was necessary. In paper III, the rat lens was sliced with a special sectioning device,[116] and PCA demonstrated a variation among the different compartments of the rat lens, separating clearly the nucleus and the equator, and nucleus from the anterior and posterior region. This was true both for UV-B exposed eye and the non-exposed eye. The anterior and the posterior cortex were distributed without any clear pattern. This might be due to the fact that the anterior and the posterior cortex are made up of the same elongated fibers. Among the quantified compounds, the most substantial metabolic changes after UV-B exposure were found in the anterior part of the lens, while the nucleus showed the smallest changes. This was consistent to the observed anterior cataract in the rat lens. Although the UV-B is exposed into the anterior part of the lens, the cellular effects seemed to be spread out in the entire lens, involving the non-exposed posterior region. Another interesting observation in paper III was that the variation in compound concentration among the

various lens compartments became smaller after exposure to UV-B. GSH and ATP/ADP were the only compounds out of 16 that had a larger concentration in the anterior portion than the nucleus after UV-B exposure. In the contralateral non-exposed lenses this was true for 13 compounds. The results presented in paper III clearly demonstrate the importance of analyzing biochemistry in distinct compartments of the lens.

CONCLUSION

In this thesis, the metabolic profiles of the rabbit aqueous humour, cornea and lens after exposure to UV-R was presented. Detection of more than 20 metabolites was performed in these tissues and in the aqueous humour. In paper III, metabolic profiles from different compartments of the rat lens was provided.

The results from this thesis show that in vivo UV-B irradiation affects metabolism of the anterior compartments of the eye. In paper I, the metabolic alteration in rabbit aqueous humour after UV-B exposure suggests several effects such as; permeability and osmoregulatory problems (alteration in betaine, glucose, valine and isoleucine), oxidation (ascorbate, formate) and deactivation of glycolytic enzymes (glucose). UV-B exposure to the rabbit cornea in paper II caused metabolic alterations that suggest similar effects; oxidation (ascorbate, hypo-taurine) and osmoregulatory problems (myo-inositol, hypo-taurine). Apoptosis (choline) and membrane disruption (choline, myo-inositol) might be additional effects on corneal tissues after UV-B radiation, interfering with cell signalling and cell transport. In the rabbit lenses in paper II, no observable metabolic alteration was observed after exposure to UV-B. UV-B absorption of the aqueous humour and the corneal tissue seems therefore to be of major protective character to the lens tissue. After exposure to UV-A radiation, there were no significant metabolic changes observed in rabbit aqueous humour (paper I), cornea or lens (paper II).

In the albino rat lenses in paper III, substantial metabolic alteration was observed after UV-B radiation. Metabolic differences were observed between the lens compartments; anterior, posterior, nucleus and the equator. An important observation was that the variation in metabolite concentration among the various lens compartments became smaller after exposure to UV-B radiation. Although the UV-B is exposed to the anterior part of the lens, the cellular damage seems to be spread throughout the whole lens, involving also the posterior region. The metabolic alterations observed in the rat lenses after UV-B exposure suggested oxidation (tyrosine, GSH, taurine, valine, isoleucine), osmotic changes (myo-inositol, taurine), and membrane dysfunction (p-choline), and are in consistence with results from

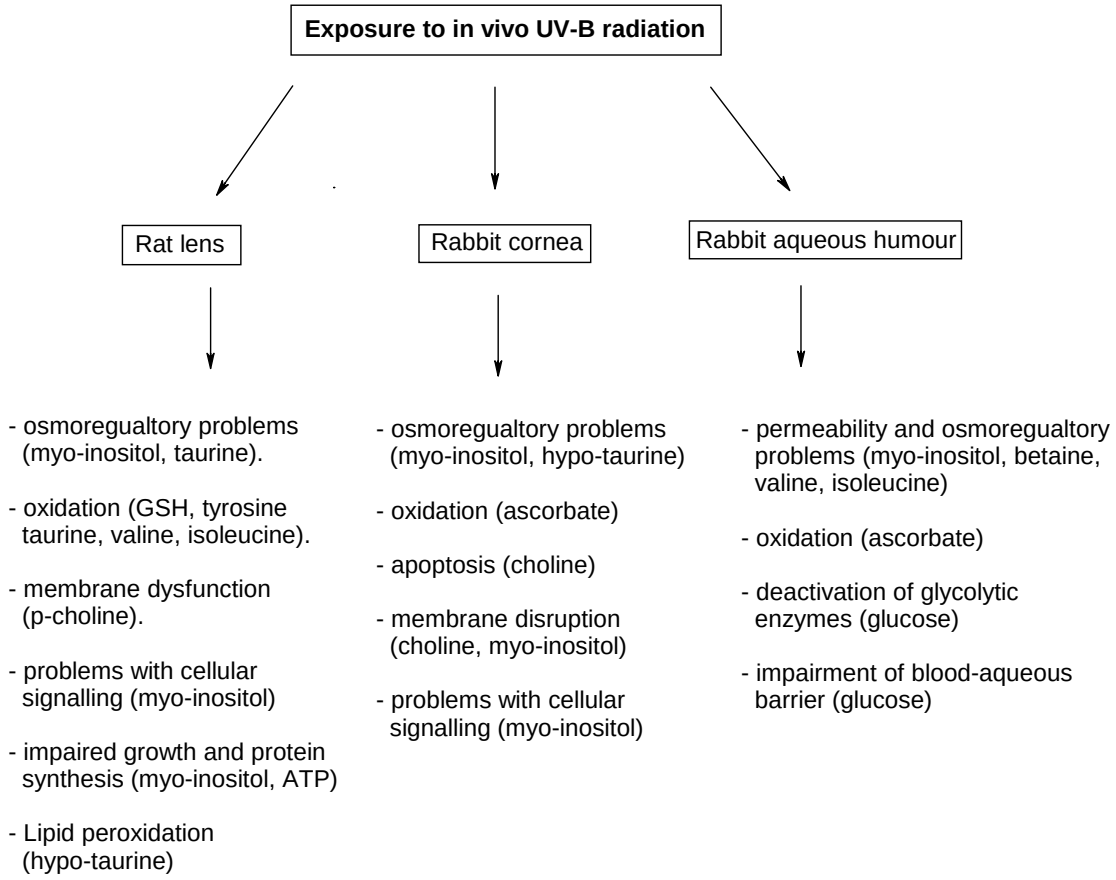

Figure 11. Suggested biochemical effects of UV-B irradiation to the anterior part of the eye. Based on results from this thesis.

aqueous humour and cornea in paper I and II. A summary of the suggested biochemical effects from exposure to UV-B radiation presented in this thesis are shown in Figure 11.

All papers in this thesis prove the effectiveness of applying NMR-based metabonomics to study UV-R exposure to the anterior compartments of the eye. HR-MAS ^{1}H NMR spectroscopy provided high quality spectra from intact corneal and lens tissues and provided important information about metabolic alteration occurring in these tissues after UV-R exposure.

Future perspectives

One of the major tasks for future studies using HR-MAS ^{1}H NMR spectroscopy is to establish a method for absolute quantification of tissue metabolites. The difficulty of finding a suitable reference compound, with no chemical interaction with the sample, has been a drawback using HR-MAS on intact tissue. A new method has recently been developed, the ERETIC (Electronic Reference To Access In Vivo Concentrations),[117,118] which can determine absolute concentrations by a electronically generated NMR signal. To be able to quantify absolute concentrations directly from intact tissue by this or other methods will be a major progress in the study of metabolism in ophthalmology.

To transfer or add the use of HR-MAS to in vivo NMR techniques for analysis of metabolic processes in living tissue would be another substantial improvement in ophthalmic research. Volume selective NMR spectroscopy allows a non-invasive, localized identification of certain chemical compounds, which have recently been shown effective in studies of the rat- and the monkey brain. If this method is developed in ophthalmology, it can identify and compare metabolic disorders and also observe long-term changes of metabolic processes in repetitive experiments. The key of this method is to localise the NMR signals to a specific volume of tissue, and in the eye, both the anterior and the posterior segments are of interest.

One of the most nearby future perspective must be to use HR-MAS ^{1}H NMR spectroscopy on human eye material. Because of the difficulty to obtain human eye material, this option is of course limited. Another task for the future metabolic studies in ophthalmology is to go into detail on chosen compounds and support the analysis with other biochemical tools to be able to detect and confirm the exact mechanisms behind the observed metabolic alterations after pathophysiological stimuli (such as UV-R exposure) or diseases. In this way, health campaigns or development of new pharmaceuticals for treatment can be initiated.

REFERENCES

1. UNEP. Ultraviolet radiation. Environmental Health Criteria 160. United Nations Environmental Programme, World Health Organization, International Commision on Non-Ionizing Radiation Protection. 1994. Geneva: WHO.
2. Ozone Secretariat UNEP. Scientific Assessment of Ozone Depletion. 2002;
3. de Gruijl FR, van der Leun JC. Environment and health: 3. Ozone depletion and ultraviolet radiation. *CMAJ*. 2000;163:851-5.
4. Congdon NG. Prevention strategies for age related cataract: present limitations and future possibillities. *Br J Ophthalmol*. 2001;85:516-520.
5. ICNIRP W, WMO, UNEP. Global solar UV Index: A practical Guide. 2002. WHO, Geneva.
6. Congdon N, Broman KW, Lai H, Munoz B, Bowie H, Gilbert D, Wojciechowski R, West SK. Cortical, but not posterior subcapsular, cataract shows significant familial aggregation in an older population after adjustment for possible shared environmental factors. *Ophthalmology*. 2005;112:73-7.
7. McCarty CA, Taylor HR. The Genetics of Cataract. *Invest Ophthalmol Vis Sci*. 2001;42:1677-1678.
8. McCarty CA, Keeffe JE, Taylor HR. The need for cataract surgery: projections based on lens opacity, visual acuity, and personal concern. *Br J Ophthalmol*. 1999;83:62-5.
9. Brian G, Taylor H. Cataract blindness-challenges for the 21st century. *Bull World Health Organ*. 2001;79:249-56.
10. Truscott RJW. Human cataract: the mechanisms responsible; light and butterfly eyes. *Int J Biochem Cell Biol*. 2003;35:1500-4.
11. Dandona L, Dandona R, Naduvilath TJ, McCarty CA, Mandal P, Srinivas M, Nanda A, Rao GN. Population-based assessment of the outcome of cataract surgery in an urban population in southern India. *Am J Ophthalmol*. 1999;127:650-8.
12. Javitt JC. Who does cataract surgery in the United States? *Arch Ophthalmol*. 1993;111:1329.
13. Kupfer C. Bowman lecture. The conquest of cataract: a global challenge. *Trans Ophthalmol Soc U K*. 1985;104 (Pt 1):1-10.

14. McCarty CA, Taylor HR. A review of the epidemiologic evidence linking ultraviolet radiation and cataracts. *Dev Ophthalmol*. 2002;35:21-31.
15. Dillon J, Zheng L, Merriam JC, Gaillard ER. The optical properties of the anterior segment of the eye: implications for cortical cataract. *Exp Eye Res*. 1999;68:785-95.
16. Pitts DG, Cullen AP, Hacker PD. Ocular effects of ultraviolet radiation from 295 to 365 nm. *Invest Ophthalmol Vis Sci*. 1977;16:932-39.
17. Söderberg PG. Experimental cataract induced by ultraviolet radiation. *Acta Ophthalmol Suppl*. 1990;1-75.
18. Hightower K, McCready J. Physiological effects of UVB irradiation on cultured rabbit lens. *Invest Ophthalmol Vis Sci*. 1992;33:1783-87.
19. Stuart DD, Cullen AP, Sivak JG, Doughty MJ. Optical effects of UV-A and UV-B radiation on the cultured bovine lens. *Curr Eye Res*. 1994;13:371-6.
20. Dillon J. Sunlight exposure and cataract. *JAMA*. 1999;281:229.
21. Linetsky M, Chemoganskiy VG, Hu F, Ortwerth BJ. Effect of UVA light on the activity of several aged human lens enzymes. *Invest Ophthalmol Vis Sci*. 2003;44:264-74.
22. Azzam N, Levanon D, Dovrat A. Effects of UV-A irradiation on lens morphology and optics. *Exp Gerontol*. 2004;39:139-46.
23. Weinreb O, Dovrat A. Transglutaminase Involvement in UV-A Damage to the Eye Lens. *Exp Eye Res*. 1996;63:591-97.
24. Čejková J, Štípek S, Crkovská J, Ardan T. Changes of superoxide dismutase, catalase and glutathione peroxidase in the corneal epithelium after UVB rays. Histochemical and biochemical study. *Histol Histopathol*. 2000;15:1043-50.
25. Schmidt J, Schmitt C, Kojima M, Hockwin O. Biochemical and morphological changes in rat lenses after long-term UV B irridation. *Ophthalmic Res*. 1992;24:317-25.
26. Michael R. Development and repair of cataract induced by ultraviolet radiation. *Ophthalmic Res*. 2000;32 Suppl 1:ii-iii; 1-44.
27. Sliney DH. Photoprotection of the eye - UV radiation and sunglasses. *J Photochem Photobiol B*. 2001;64:166-75.
28. Coroneo MT, Muller-Stolzenburg NW, Ho A. Peripheral light focusing by the anterior eye and the ophthalmohelioses. *Ophthalmic Surg*. 1991;22:705-11.

29. Sasaki H, Kawakami Y, Ono M, Jonasson F, Shui YB, Cheng HM, Robman L, McCarty C, Chew SJ, Sasaki K. Localization of cortical cataract in subjects of diverse races and latitude. *Invest Ophthalmol Vis Sci*. 2003;44:4210-4.
30. Rosenthal FS, Phoon C, Bakalian AE, Taylor HR. The ocular dose of ultraviolet radiation to outdoor workers. *Invest Ophthalmol Vis Sci*. 1988;29:649-56.
31. Boettner EA, Wolter JR. Transmission of the ocular media. *Invest Ophthalmol*. 1962;1:776-83.
32. Harding JJ. Biochemistry of the eye. 1997. London: Chapman & Hall Medical. 1st ed.
33. Forrester JD, AD. McMenamin PG. Lee, WR. The eye: basic sciences in practice. 2002. London: Saunders, 2nd ed.
34. Podskochy A. Protective role of corneal epithelium against ultraviolet radiation damage. *Acta Ophthalmol Scand*. 2004;82:714-7.
35. Podskochy A, Gan L, Fagerholm P. Apoptosis in UV-exposed rabbit corneas. *Cornea*. 2000;19:99-103.
36. Ringvold A, Davanger M. Changes in the rabbit corneal stroma caused by UV-radiation. *Acta Ophthalmol (Copenh)*. 1985;63:601-6.
37. Gray RH, Johnson GJ, Freedman A. Climatic droplet keratopathy. *Surv Ophthalmol*. 1992;36:241-53.
38. Moran DJ, Hollows FC. Pterygium and ultraviolet radiation: a positive correlation. *Br J Ophthalmol*. 1984;68:343-6.
39. Klintworth GK. The cornea-structure and macromolecules in health and disease. A review. *Am J Pathol*. 1977;89:718-808.
40. Ringvold A. Aqueous humour and ultraviolet radiation. *Acta Ophthalmol*. 1980;58:69-82.
41. Ringvold A. The significance of ascorbate in the aqueous humour protection against UV-A and UV-B. *Exp Eye Res*. 1996;62:261-64.
42. Berman ER. Biochemistry of the eye. 1991. New York: plenum press. 1st ed.
43. Kaufman PL, Alm A. Adlers`s physiology of the eye. 2003. St. Louis: Mosby, 10th ed.
44. Graymore C. Biochemistry of the eye. 1970. London: Academic Press Inc. 1st ed.

45. Hockwin O, Kojima M, Müller-Breitenkamp U, Wegener A. Lens and cataract research of the 20th century: a review of results, errors and misunderstandings. *Dev Ophthalmol*. 2002;35:1-11.

46. ICNIRP. ICNIRP Guidelines on limits of exposure to UV radiation of wavelengths between 180 nm and 400 nm (incoherent optical radiation). *Health Physics*. 2004;87:171-186.

47. Söderberg PG, Michael R, Merriam JC. Maximum acceptable dose of ultraviolet radiation: a safety limit for cataract. *Acta Ophthalmol Scand*. 2003;81:165-9.

48. Rose RC, Richer SP, Bode AM. Ocular oxidants and antioxidant protection. *Proc Soc Exp Biol Med*. 1998;217:397-407.

49. Simpson GL, Ortwerth BJ. The non-oxidative degradation of ascorbic acid at physiological conditions. *Biochim Biophys Acta*. 2000;1501:12-24.

50. Ringvold A. Corneal epithelium and UV-protection of the eye. *Acta Ophthalmol Scand*. 1998;76:149-53.

51. Giblin FJ. Glutathione: a vital lens antioxidant. *J Ocul Pharmacol Ther*. 2000;16:121-35.

52. Risa Ø, Sæther O, Löfgren S, Söderberg PG, Krane J, Midelfart A. Metabolic changes in rat lens after in vivo exposure to ultraviolet irradiation: measurements by high resolution MAS ^{1}H NMR spectroscopy. *Invest Ophthalmol Vis Sci*. 2004;45:1916-21.

53. Midelfart A, Dybdahl A, Gribbestad IS. Detection of different metabolites in the rabbit lens by high resolution ^{1}H NMR spectroscopy. *Curr Eye Res*. 1996;15:1175-81.

54. Midelfart A, Dybdahl A, Gribbestad IS. Metabolic analysis of the rabbit cornea by proton nuclear magnetic resonance spectroscopy. *Ophthalmic Res*. 1996;28:319-29.

55. Gribbestad IS, Midelfart A. High-resolution ^{1}H NMR spectroscopy of aqueous humour from rabbits. *Graefes Arch Clin Exp Ophthalmol*. 1994;232:494-98.

56. Nishikawa Y, Kurata T. Interconversion between dehydro-L-ascorbic acid and L-ascorbic acid. *Biosci Biotechnol Biochem*. 2000;64:476-83.

57. Sæther O, Risa Ø, Čejková J, Krane J, Midelfart A. High-resolution magic angle spinning ^{1}H NMR spectroscopy of metabolic changes in rabbit lens after

treatment with dexamethasone combined with UVB exposure. *Graefes Arch Clin Exp Ophthalmol*. 2004;242:1000-7.

58. Sæther O, Krane J, Risa Ø, Čejková J, Midelfart A. High-resolution MAS ^{1}H NMR spectroscopic analysis of rabbit cornea after treatment with Dexamethasone and exposure to UVB radiation. *Curr Eye Res*. 2005;30:1041-49.

59. Risa Ø, Sæther O, Kakar M, Mody V, Löfgren S, Söderberg PG, Krane J, Midelfart A. Time dependency of metabolic changes in rat lens after in vivo UVB irradiation analysed by HR-MAS ^{1}H NMR spectroscopy. *Exp Eye Res*. 2005;81:407-14.

60. Trayhurn P, Heyningen RV. The metabolism of glutamine in the bovine lens: glutamine as a source of glutamate. *Exp Eye Res*. 1973;17:149-154.

61. Cotman CW, Monaghan DT. Anatomical organization of excitatory amino acid receptors and their properties. *Adv Exp Med Biol*. 1986;203:237-52.

62. Tadolini B, Pintus G, Pinna GG, Bennardini F, Franconi F. Effects of taurine and hypotaurine on lipid peroxidation. *Biochem Biophys Res Commun*. 1995;213:820-6.

63. Aruoma OI, Halliwell B, Hoey BM, Butler J. The antioxidant action of taurine, hypotaurine and their metabolic precursors. *Biochem J*. 1988;256:251-5.

64. Ricci G, Dupre S, Federici G, Spoto G, Matarese RM, Cavallini D. Oxidation of hypotaurine to taurine by ultraviolet irradiation. *Physiol Chem Phys*. 1978;10:435-41.

65. Shioda R, Reinach PS, Hisatsune T, Miyamoto Y. Osmosensitive taurine transporter expression and activity in human corneal epithelial cells. *Invest Ophthalmol Vis Sci*. 2002;43:2916-22.

66. Cammarata PR, Schafer G, Chen SW, Guo Z, Reeves RE. Osmoregulatory alteration in taurine uptake by cultured human and bovine lens epithelial cells. *Invest Ophthalmol Vis Sci*. 2002;43:425-33.

67. Devamanoharan PS, Ali AH, Varma SD. Oxidative stress to rat lens in vitro: protection by taurine. *Free Radic Res*. 1998;29:189-95.

68. Löfgren S, Söderberg PG. Rat lens glycolysis after in vivo exposure to narrow band UV or blue light radiation. *J Photochem Photobiol B Biology*. 1995;30:145-51.

69. Löfgren S, Söderberg PG. Lens lactate dehydrogenase inactivation after UV-B irradiation: An in vivo measure of UVR-B penetration. *Invest Ophthalmol Vis Sci*. 2001;42:1833-36.

70. Zeisel SH, Mar MH, Howe JC, Holden JM. Concentrations of choline-containing compounds and betaine in common foods. *J Nutr*. 2003;133:1302-7.

71. Jernigan HM, Jr., Ekambaram MC, Blum PS, Blanchard MS. Effect of xylose on the synthesis of phosphorylcholine and phosphorylethanolamine in rat lenses. *Exp Eye Res*. 1993;56:291-7.

72. Jernigan HM, Jr., Desouky MA, Geller AM, Blum PS, Ekambaram MC. Efflux and hydrolysis of phosphorylethanolamine and phosphorylcholine in stressed cultured rat lenses. *Exp Eye Res*. 1993;56:25-33.

73. Yokoyama T, Lin LR, Chakrapani B, Reddy VN. Hypertonic stress increases NaK ATPase, taurine, and myoinositol in human lens and retinal pigment epithelial cultures. *Invest Ophthalmol Vis Sci*. 1993;34:2512-17.

74. Zhou C, Agarwal N, Cammarata PR. Osmoregulatory alterations in myo-inositol uptake by bovine lens epithelial cells. Part 2: Cloning of a 626 bp cDNA portion of a Na^+/myo-inositol cotransporter, an osmotic shock protein. *Invest Ophthalmol Vis Sci*. 1994;35:1236-42.

75. Jiang Z, Chung SK, Zhou C, Cammarata PR, Chung SSM. Overexpression of Na^+-dependent myo-inositol transporter gene in mouse lens led to congenital cataract. *Invest Ophthalmol Vis Sci*. 2000;41:1467-72.

76. Wada E, Matsuzawa A, Takenawa T, Tsumita T. Myo-inositol content of the lens in hereditary cataract mice. *Exp Eye Res*. 1978;26:119-22.

77. Mayr GW. Inositol phosphates: structural components, regulators and signal transducers of the cell - a review. *Top Biochem*. 1988;7:1-18.

78. Claridge TDW. High-resolution NMR techniques in organic chemistry. 1999. Tetrahedron organic chemistry series volume 19. Oxford; Pergamon, 1st ed.

79. Nicholson JK, Foxall PJD, Spraul M, Farrant RD, Lindon JC. 750 MHz ^1H and ^1H-^{13}C NMR spectroscopy of human blood plasma. *Anal Chem*. 1995;67:793-811.

80. Lindon JC, Nicholson JK, Everett JR. NMR spectroscopy of biofluids. *Annu Rep NMR Spectros*. 1999;38:1-88.

81. Garrod S, Humpfer E, Spraul M, Connor SC, Polley S, Connelly J, Lindon JC, Nicholson JK, Holmes E. High-resolution magic angle spinning ^{1}H NMR spectroscopic studies on intact rat renal cortex and medulla. *Magn Reson Med*. 1999;41:1108-18.

82. Rooney OM, Troke J, Nicholson JK, Griffin JL. High-resolution diffusion and relaxation-edited magic angle spinning ^{1}H NMR spectroscopy of intact liver tissue. *Magn Reson Med*. 2003;50:925-30.

83. Bollard ME, Murray AJ, Clarke K, Nicholson JK, Griffin JL. A study of metabolic compartmentation in the rat heart and cardiac mitochondria using high-resolution magic angle spinning ^{1}H NMR spectroscopy. *FEBS Lett*. 2003;553:73-78.

84. Cheng LL, Ma MJ, Becerra L, Ptak T, Tracey I, Lackner A, Gonzalez RG. Quantitative neuropathology by high resolution magic angle spinning proton magnetic resonance spectroscopy. *Proc Natl Acad Sci U S A*. 1997;94:6408-13.

85. Sitter B, Autti T, Tyynela J, et al. High-resolution magic angle spinning and ^{1}H magnetic resonance spectroscopy reveal significantly altered neuronal metabolite profiles in CLN1 but not in CLN3. *J Neurosci Res*. 2004;77:762-9.

86. Sitter B, Lundgren S, Bathen TF, Halgunset J, Fjosne HE, Gribbestad IS. Comparison of HR MAS MR spectroscopic profiles of breast cancer tissue with clinical parameters. *NMR Biomed*. 2005.; In press.

87. Sitter B, Sonnewald U, Spraul M, Fjösne HE, Gribbestad IS. High-resolution magic angle spinning MRS of breast cancer tissue. *NMR Biomed*. 2002;15:327-37.

88. Sitter B, Bathen T, Hagen B, Arentz C, Skjeldestad FE, Gribbestad IS. Cervical cancer tissue characterized by high-resolution magic angle spinning MR spectroscopy. *MAGMA*. 2004;16:174-81.

89. Meiboom S, Gill D. Modified spin-echo method for measuring nuclear relaxation times. *Rev Sci Instrum*. 1958;29:688-91.

90. Bollard ME, Garrod S, Holmes E, Lindon JC, Humpfer E, Spraul M, Nicholson JK. High-resolution ^{1}H and ^{1}H-^{13}C magic angle spinning NMR spectroscopy of rat liver. *Magn Reson Med*. 2000;44:201-7.

91. Fan TW-M. Metabolite profiling by one- and two-dimensional NMR analysis of complex mixtures. *Prog NMR Spectrosc*. 1996;28:161-219.

92. Risa Ø, Sæther O, Midelfart A, Krane J, Čejková J. Analysis of immediate changes of water-soluble metabolites in alkali-burned rabbit cornea, aqueous humour and lens by high-resolution ^{1}H-NMR spectroscopy. *Graefes Arch Clin Exp Ophthalmol*. 2002;240:49-55.

93. Nicholson JK, Lindon JC, Holmes E. 'Metabonomics': understanding the metabolic responses of living systems to pathophysiological stimuli via multivariate statistical analysis of biological NMR spectroscopic data. *Xenobiotica*. 1999;29:1181-9.

94. Lindon JC, Holmes E, Nicholson JK. So what`s the deal with metabonomics? *Anal Chem*. 2003;75:384-91.

95. Reo NV. NMR-based metabolomics. *Drug Chem Toxicol*. 2002;25:375-82.

96. Ansari AS, Tahib S, Ali R. Degradation of phenylalanine in the presence of hydrogen peroxide. *Experientia*. 1976;32:573-4.

97. Stryer L. Biochemistry. 1995. New York: W.H. Freeman and Company, 4th ed.

98. De Berardinis E, Tieri O, Polzella A, Iuglio N. The chemical composition of the human aqueous humour in normal and pathological conditions. *Exp Eye Res*. 1965;4:179-86.

99. Malorny G, Rietbrock N, Schneider M. Die oxydation des formaldehyds zu ameisensäure im blut, ein beitrag zum stoffwechsel des formaldehyds. *Naunyn Schmiedebergs Arch Pharmacol*. 1965;250:419-36.

100. Deacon R, Perry J, Lumb M, Chanarin I. Formate metabolism in the cobalamin-inactivated rat. *Br J Haematol*. 1990;74:354-59.

101. Barclay BJ. B complex vitamin compositions that protect against cellular damage caused by ultraviolet light. 2002. *WO 2002003942*.

102. Nicholls P. The effect of formate on cytochrome aa3 and on electron transport in the intact respiratory chain. *Biochim Biophys Acta*. 1976;430:13-29.

103. Treichel JL, Henry MM, Skumatz CMB, Eells JT, Burke JM. Formate, the toxic metabolite of methanol, in cultured ocular cells. *NeuroToxicology*. 2003;24:825-34.

104. Reddy VN. Glutathione and its function in the lens-an overview. *Exp Eye Res*. 1990;50:771-8.

105. Spector A. Oxidative stress-induced cataract: mechanism of action. *FASEB J*. 1995;9:1173-82.

106. Yancey PH, Clark ME, Hand SC, Bowlus RD, Somero GN. Living with water stress: evolution of osmolyte systems. *Science*. 1982;217:1214-22.

107. Zigman S. Environmental near-UV radiation and cataracts. *Optom Vis Sci*. 1995;72:899-901.

108. Michael R, Söderberg PG, Chen E. Dose-response function for lens forward light scattering after in vivo exposure to ultraviolet radiation. *Graefes Arch Clin Exp Ophthalmol*. 1998;236:625-9.

109. Michael R, Söderberg PG, Chen E. Long-term development of lens opacities after exposure to ultraviolet radiation at 300 nm. *Ophthalmic Res*. 1996;28:209-18.

110. Dong X, Ayala M, Löfgren S, Söderberg PG. Ultraviolet radiation-induced cataract: age and maximum acceptable dose. *Invest Ophthalmol Vis Sci*. 2003;44:1150-4.

111. Dong X, Löfgren S, Ayala M, Söderberg PG. Maximum tolerable dose for avoidance of cataract induced by ultraviolet radiation-B for 18 to 60 week old rats. *Exp Eye Res*. 2005;80:561-6.

112. Löfgren S, Michael R, Söderberg PG. Impact of age and sex in ultraviolet radiation cataract in the rat. *Invest Ophthalmol Vis Sci*. 2003;44:1629-33.

113. Diestelhorst M, Krieglstein G. The effect of trabeculectomy on the aqueous humor flow of the unoperated fellow eye. *Graefes Arch Clin Exp Ophthalmol*. 1991;229:274-6.

114. Mietz H, Jacobi PC, Welsandt G, Krieglstein GK. Trabeculectomies in fellow eyes have an increased risk of tenon's capsule cysts. *Ophthalmology*. 2002;109:992-7.

115. Ringvold A, Anderssen E, Kjonniksen I. Ascorbate in the corneal epithelium of diurnal and nocturnal species. *Invest Ophthalmol Vis Sci*. 1998;39:2774-7.

116. Bessems GJ, Dragomirescu V, Moller B, Korte I, Hockwin O. Biochemical analysis of bovine lens sections obtained by a new sectioning device. *Lens Eye Toxic Res*. 1989;6:175-82.

117. Pfeuffer J, Juchem C, Merkle H, Nauerth A, Logothetis NK. High-field localized ^{1}H NMR spectroscopy in the anesthetized and in the awake monkey. *Magn Reson Imaging*. 2004;22:1361-72.

118. Pfeuffer J, Tkac I, Provencher SW, Gruetter R. Toward an in vivo neurochemical profile: quantification of 18 metabolites in short-echo-time ^{1}H NMR spectra of the rat brain. *J Magn Reson*. 1999;141:104-20.